Nano Energy 153 (2026) 111944

Contents lists available at ScienceDirect

Nano Energy

journal homepage: www.elsevier.com/locate/nanoen

Review

From contact electrification to chemical reactions: The emergence of contact-electro-catalysis

Han Qian [a,b], Zhong Lin Wang [a,*], Di Wei [a,*]

[a] Beijing Institute of Nanoenergy and Nanosystems, Chinese Academy of Sciences, Beijing 101400, China
[b] School of Nanoscience and Engineering, University of Chinese Academy of Sciences, Beijing 100049, China

ARTICLE INFO

Keywords:
Contact electrification
Interfacial charge transfer
Contact-electro-catalysis (CEC)
Interfacial microenvironment
Electrical double layer (EDL)

ABSTRACT

Contact electrification, a ubiquitous interfacial phenomenon recognized for centuries, has recently been identified as a previously underexplored driving force for chemical reactivity. Beyond its classical roles in electrostatics and energy harvesting, charge transfer and accumulation at contacting interfaces can generate strong interfacial electric fields and reactive radical species, which collectively initiate and sustain chemical reactions. This Review establishes contact-electro-catalysis (CEC) as a conceptual framework for chemical transformations governed by interfacial charge transfer, rather than by externally applied electrical, light, or thermal stimuli. We focus on the intrinsic coupling between interfacial charge transfer, the local interfacial microenvironment, and reaction pathways. Representative CEC-enabled processes are surveyed, including organic pollutant degradation, biomedical applications, direct synthesis of H_2O_2, activation of gas molecules, reduction of metal ions, and recycling of spent lithium-ion batteries. These examples highlight defining attributes of CEC, such as electrode-free operation, broad materials generality, and the spatiotemporal decoupling of paired redox reactions. We conclude by assessing the current predominance and relative balance of oxidation versus reduction reactions reported in CEC, analyzing the underlying mechanistic origins of this disparity, and articulating key scientific challenges and emerging opportunities, before proposing a future roadmap that positions CEC as a versatile and sustainable platform for chemical transformations.

1. Introduction

Contact electrification (CE) is one of the earliest recognized interfacial phenomena, with origins tracing back to ancient observations of rubbed amber attracting lightweight objects [1–4]. With the development of classical physics, it was formalized as charge transfer and accumulation occurring during contact and separation between dissimilar materials and was long regarded as a macroscopic electrostatic effect [5–7]. Although CE is ubiquitous at diverse interfaces, it has long remained largely disconnected from mainstream chemical research and has seldom been recognized as a viable driving force for chemical reactions [8,9]. This long-standing neglect stems largely from conventional chemical paradigms, in which reactions are classified and regulated by externally imposed energy inputs, such as electric fields in electrochemistry, photons in photochemistry, or thermal activation in thermochemistry [10–15]. By contrast, previous studies on liquid-solid CE primarily attributed charge transfer solely to ion adsorption or ionizations [16–20]. Occurring in the absence of electrodes or stable external fields, such processes were therefore widely regarded as chemically insignificant [21]. As a consequence, CE has historically been relegated to applications in electrostatic control, powder handling and, more recently, energy harvesting, while its potential role as a genuine interfacial driving force for chemical reactions has remained largely overlooked [22–26].

The mechanisms underlying CE are diverse and strongly system-dependent [2,27]. Depending on the contacting materials and interfacial environment, charge separation may involve electron transfer, ion transfer, or material transfer processes [4,28,29]. Earlier studies have highlighted ion partitioning in adsorbed water layers [4], charge-penetration-depth-dependent contributions from electrons and ions [28], and mechanically induced ionic fragment formation [29]. Recently, a series of studies have demonstrated the existence of electron transfer during CE at liquid-solid interfaces, and in some cases, electron transfer has been identified as the dominant process [2,30]. To account for this mechanism, an “electron-cloud-potential-well” model has been proposed, which attributes interfacial electron transfer in CE to the

* Corresponding authors.
E-mail addresses: zlwang@binn.cas.cn (Z.L. Wang), weidi@binn.cas.cn (D. Wei).

https://doi.org/10.1016/j.nanoen.2026.111944
Received 17 March 2026; Received in revised form 2 April 2026; Accepted 8 April 2026
Available online 9 April 2026

overlap of electronic clouds induced by mechanical stimulation [16]. Specifically, driven by thermal motion or fluid pressure, liquid molecules collide with solid surfaces, thereby inducing electron cloud overlap that enables electron exchange. Building on this concept, Wang et al. [2] proposed a hybrid electrical double layer (EDL) model that incorporates both electron transfer and ion adsorption effects, in which EDL formation can be described as a "two-step" process (Fig. 1a). In the first step, molecules and ions in the liquid collide with the solid surface under thermal motion or fluid pressure. Owing to the overlap of electronic clouds, electrons are exchanged across the solid-liquid interface, while ions are simultaneously adsorbed onto the solid surface (Fig. 1b). This step accounts for the origin and composition of the initial surface charges, which remain ambiguous in conventional EDL models. In the second step, analogous to the classical EDL framework, free ions in the liquid are electrostatically attracted to the charged solid surface, leading to the formation of the EDL. Crucially, the nature of electron transfer or excitation as the primary driving force delineates distinct chemical reaction paradigms. In electrochemical systems, reactive electrons are supplied through charge exchange at electrodes, whereas in photochemical processes, photoexcitation generates electron-hole pairs that initiate reactivity. By extension, the presence of electron transfer during CE implies that CE-induced charge separation can, in principle, serve as a viable driving force for chemical reactions. We refer to this process as contact-electro-catalysis (CEC), which serves as a conceptual bridge between CE and mechanochemistry and has been proposed as an important complement to existing reaction strategies.

In this review, we articulate the conceptual framework, underlying principles, defining characteristics, representative applications, and prospective directions of CEC. By integrating recent advances with emerging mechanistic insights, we provide a coherent and comprehensive perspective on CEC as a distinct, versatile, and sustainable chemical paradigm. We anticipate that this review will not only offer an authoritative overview of current progress but also stimulate further critical thinking, methodological innovation, and transformative developments in this rapidly evolving field.

2. Fundamentals of CEC

From a fundamental physico-chemical perspective, CEC is governed by three tightly coupled elements: interfacial charge transfer and accumulation, the establishment of intense interfacial electric fields, and the generation of reactive radical species, which act synergistically to initiate and drive chemical reactions [2]. Wang et al. [31] first proposed a "two-step" reaction model for CEC in aqueous systems, involving the oxidation of water and the reduction of oxygen molecules. Taking fluorinated ethylene propylene (FEP) as a representative material, in the first step, electrons are transferred from water molecules to FEP upon contact, resulting in the formation of hydronium cations (H_3O^+) and hydroxyl radicals (•OH). The electron-accepting state of FEP after acquiring electrons from water molecules is denoted as FEP*. In the second step, when dissolved oxygen in the aqueous solution comes into contact with FEP*, electrons stored on FEP* are transferred to oxygen molecules, leading to the formation of superoxide radicals ($•O_2^-$). Meanwhile, FEP returns to its initial uncharged state, thereby completing the reaction cycle. Subsequently, Wei et al. [32] extended this model to non-protic organic systems, in which the first step is transformed into the oxidation of organic solvent molecules. Taking dimethyl sulfoxide (DMSO) as an example, electron transfer from DMSO to FEP results in the formation of methyl radicals ($•CH_3$), while the second step remains analogous to that observed in aqueous systems. In addition, excess electrons accumulate at the interface during CE, giving rise to high-intensity triboelectric fields on the charged surface [33,34]. These interfacial electric fields can significantly influence the interfacial microenvironment by polarizing interfacial solvent molecules, reorganizing hydrogen-bond networks, redistributing ions, lowering activation barriers, facilitating electron transfer, and stabilizing reactive intermediates [35–38].

Existing studies have systematically demonstrated that CEC is not confined to a single experimental condition, but rather represents a general class of interfacial chemical processes driven by mechanically induced contact-separation events. In principle, various modes of mechanical stimulation, including vibration, sliding, collision, grinding, and ultrasonication, can trigger CEC by enabling repeated interfacial

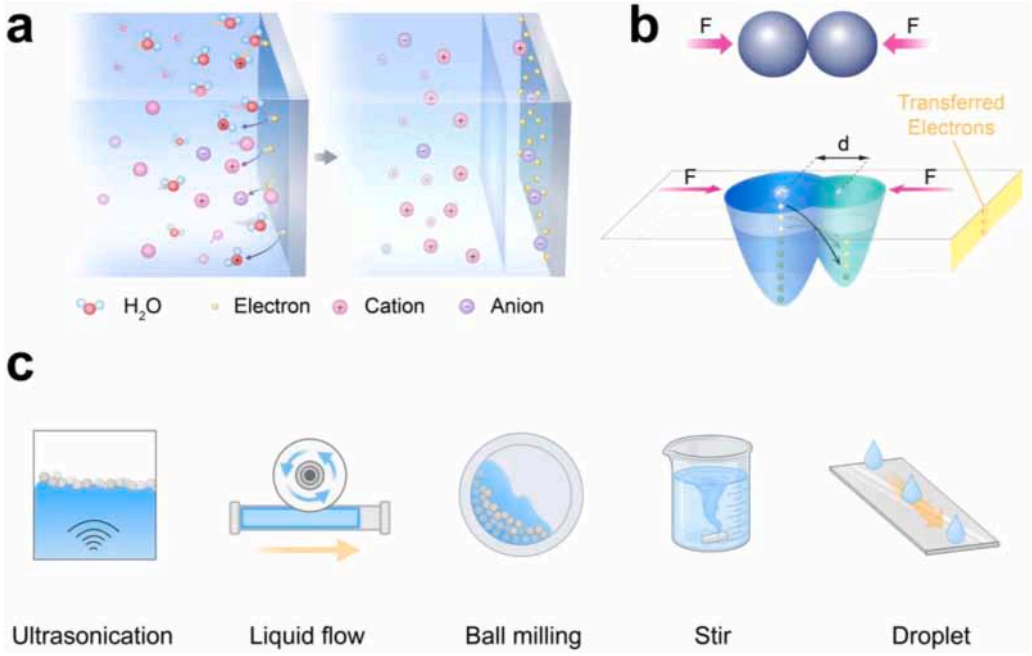

Fig. 1. Fundamentals of contact-electro-catalysis (CEC). (a) Wang's hybrid EDL model and its "two-step'' formation process. (b) The electron-cloud-potential well model to elucidate a generalized scenario of contact-electrification between two materials. Reproduced with permission [16]. Copyright 2024, The Royal Society of Chemistry. (c) Common types of mechanical stimulation for CEC.

contact-separation [39–43]. At present, ultrasonication, liquid flow, ball milling, stir, and macroscopic droplet motion represent commonly employed and effective strategies, as they provide interfacial contact events with sufficient frequency and energy to facilitate charge transfer (Fig. 1c). Meanwhile, CEC exhibits a high degree of tolerance toward material form and length scale, with reactive interfaces spanning from nanoscale powders and micrometer-scale emulsions to millimeter-scale spheres and centimeter-scale films [33,44,45]. In terms of material composition, strongly triboelectric polymers, inorganic oxides, semiconductors, and their composite systems have been demonstrated to exhibit chemical reactivity, among which surface fluorination, as a strategy for modulating interfacial electronic structure, plays a critical role in enhancing CEC efficiency [46–48]. Further studies indicate that operational parameters, including ultrasonic frequency and power, ball-milling speed, liquid flow rate, and temperature, exert significant influences on CEC processes, revealing that CEC is intrinsically highly sensitive to interfacial mechanical energy input [47,49,50].

Compared with conventional chemical reaction systems driven by externally applied electric, light, or thermal fields, CEC exhibits a series of intrinsic and distinctive advantages. First, CEC operates without external fields, as its chemical driving forces originate from spontaneous charge transfer and interfacial electric fields generated during contact-separation processes [51,52]. This fundamentally eliminates reliance on electrodes, power supplies, light sources, or bulk heating, thereby simplifying reaction systems and reducing both energy input and device complexity. Second, CEC typically enables chemical transformations under mild reaction conditions [36,53]. Because reaction activation is confined to highly localized interfacial regions, the resulting intense electric fields and reactive radical species can significantly lower activation barriers and steer reaction pathways at micro- and nanoscale dimensions. Consequently, harsh conditions, such as elevated temperatures, high pressures, or strongly oxidizing/reducing environments, are unnecessary, offering particular advantages for thermally sensitive molecules and complex systems. Third, CEC exhibits remarkable material universality [16,54]. Unlike conventional catalysts, interfacial charge generation occurs largely independently of the material type, electronic band structure, or the presence of noble metals. A broad spectrum of inorganic oxides, semiconductors, polymers, and fluorinated liquids can serve as reactive platforms. This minimal material dependence substantially expands the accessible material space and facilitates the development of low-cost, scalable reaction systems. Fourth, the functional materials involved in CEC generally exhibit good cycling stability [7,16,55]. Because the underlying mechanism depends on interfacial charge regulation rather than chemical consumption of the material, structural degradation and activity loss are minimal, enabling stable performance over repeated contact cycles. This contrasts with the deactivation commonly observed in conventional catalytic systems. Moreover, the energy input for CEC is broadly available and readily accessible [56–58]. Mechanical energy acts as the primary driving stimulus and can be harvested from a wide array of sources, including ultrasonication, vibration, friction, fluid flow, ball milling, and even ambient environmental perturbations. This versatility and ease of integration confer substantial flexibility for practical implementation. Simultaneously, CEC allows spatiotemporal decoupling of paired redox reactions [59]. In this paradigm, charge transfer, accumulation, and chemical transformation occur transiently within localized interfacial regions, rather than being restricted to fixed electrode surfaces or steady-state reaction zones. This spatiotemporal decoupling provides unique opportunities to control reaction selectivity, spatial confinement, and kinetic pathways, capabilities that are challenging to achieve with conventional reaction architectures. Importantly, CEC also demonstrates significant potential as a green and environmentally sustainable approach [6,8]. By minimizing external energy inputs, relaxing material constraints, and eliminating the need for harsh or complex reaction conditions, CEC offers the potential for substantially higher overall energy and resource efficiency compared with conventional reaction schemes. Crucially, CEC is not merely a replacement for existing chemical strategies; rather, it constitutes a complementary and synergized paradigm defined by its unique driving-force origin, reaction modality, and system design, opening new avenues to expand the scope of chemical transformations and advance sustainable chemical processes [31].

3. Applications of CEC

3.1. Organic pollutant degradation

Organic pollutant degradation represents one of the most representative and systematically investigated application areas of CEC [33,48,60]. A wide variety of organic pollutants are ubiquitously present in aquatic environments, including organic dyes [31,47,49,61], phenolic pollutants [62–64], antibiotics [65–67], sulfadiazine [68,69], and perfluoroalkyl substances [35,36]. These pollutants generally exhibit diverse molecular structures, complex reaction pathways, and strong environmental persistence, making them difficult to remove efficiently using conventional physical separation or traditional chemical oxidation methods [69–71]. Recent studies have demonstrated that CEC can operate without external electric fields, light excitation, or elevated temperatures, and can instead generate reactive species such as •OH and $\bullet O_2^-$ radicals through electron transfer and strong localized electric fields induced during interfacial contact-separation processes [31,49]. Owing to its broad material compatibility and reusability, and without relying on noble metals or specific semiconductor catalysts, CEC significantly reduces energy input and the risk of undesired side reactions, thereby exhibiting unique advantages and considerable potential for the treatment of complex organic pollutants.

3.1.1. Organic dye degradation

Organic dyes are among the earliest studied and most representative classes of organic pollutants in industrial wastewater [42,45,48,72]. Owing to their well-defined molecular structures and sensitive spectroscopic responses, they are frequently employed as model systems for evaluating emerging degradation strategies [31,50,73,74]. In studies of CEC, methyl orange (MO) has been widely adopted as a standard probe molecule, systematically promoting the transition of this field from an interfacial physical phenomenon to a designable chemical reaction pathway [31,34,44,49]. At the proof-of-concept stage, Wang et al. [31] reported that FEP particles can generate reactive oxygen species (ROS) in aqueous media through CE with water and dissolved oxygen, thereby achieving complete degradation of MO within approximately 3 h (Fig. 2a-c). This mechanism was shown to be applicable to multiple dielectric materials, preliminarily establishing a reaction paradigm in which CEC can directly drive oxidative degradation of dyes. Moreover, CEC is not restricted to a single mode of mechanical stimulation but instead represents a general reaction process that is highly sensitive to interfacial contact-separation events. Beyond ultrasonic cavitation, efficient MO degradation has been realized under various mechanical conditions, including ball-milling, microdroplet contact, and liquid-phase stirring. For example, Wang et al. [49] demonstrated that triboelectric polymers such as polytetrafluoroethylene (PTFE) and polydimethylsiloxane (PDMS) can induce interfacial charge transfer during liquid-assisted ball milling, enabling the in situ generation of ROS and rapid degradation of MO (Fig. 2d-e). Notably, PTFE balls exhibited the highest CE capability, followed by PDMS, whereas the polypropylene (PP) balls removed only 3.1% of MO, indicating an almost negligible ability to extract electrons from water (Fig. 2f). The strong correlation between CE capability and degradation rate further confirms that ROS generated via CE are responsible for dye degradation. Similarly, in microdroplet systems, liquid–solid contact can also trigger dye degradation: electron transfer induced by water droplets sliding over PTFE surfaces generates ROS, enabling ultrafast degradation of organic dyes such as crystal violet, with 90% removal achieved within 38 s [43]. In

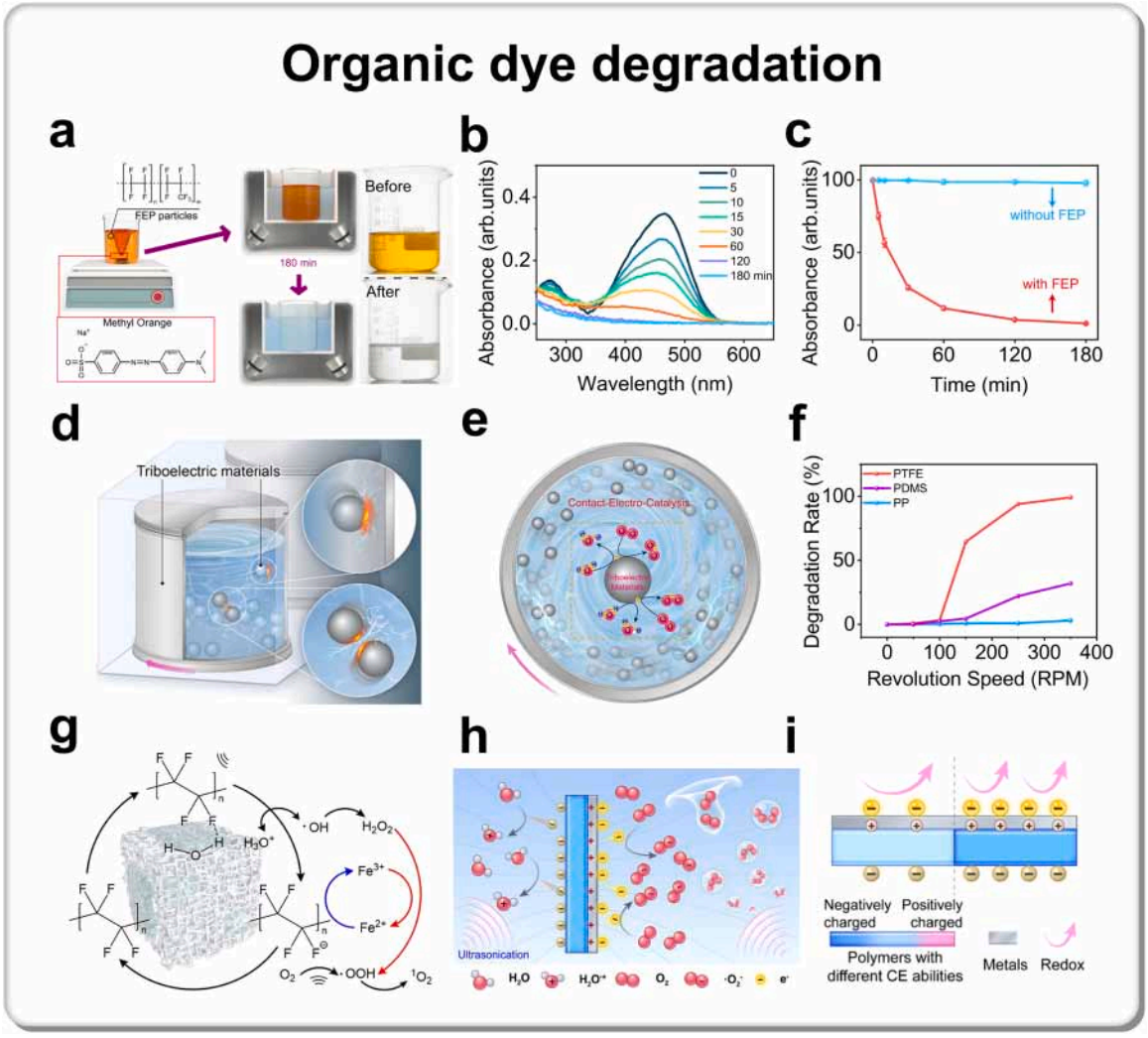

Fig. 2. Applications of CEC: organic pollutant degradation (organic dye degradation). (a) Schematic of the experimental setup and protocol for the degradation of methyl orange. (b) Ultraviolet-visible (UV-Vis) spectra of methyl orange solution during ultrasonication in presence of FEP powder (20 mg) for 3 h. (c) Comparison of absorbance of methyl orange solution between situations of with/without FEP powder. Reproduced with permission [31]. Copyright 2022, Springer Nature. (d) Schematic illustration of a ball mill process using triboelectric materials. (e) Proposed working principle of CEC during ball milling using triboelectric materials. The gray circle represents for milling balls made of triboelectric materials, pink circle for O atoms, purple circle for H atoms, and yellow circle for electrons. (f) Comparison of degradation rate when different triboelectric materials were utilized. PP is short for polypropylene, and PDMS for polydimethylsiloxane. The size of milling balls is 5 mm in this investigation. Reproduced with permission [49]. Copyright 2022, Springer Nature. (g) Pathway diagram of active oxygen species generation through water oxidation, oxygen reduction, and Fe^{III} cycling in the system. Reproduced with permission [75]. Copyright 2025, Wiley. (h) Electron transfer principle for Janus composites. The delivery of charges on the metal surface is enhanced via the modulation with polymers. (i) Effect of polymer electrification on the induced charge at the metal end. The high charge accumulation ability of polymers induces large amounts of induced charges. Reproduced with permission [34]. Copyright 2024, American Chemical Society.

addition, by introducing PTFE coatings onto waste textiles, low-frequency friction driven solely by conventional stirring can realize 91.5% degradation of Rhodamine B within 24 h [47]. Collectively, these studies demonstrate that CEC can be universally induced across multiple length scales and mechanical modalities.

In studies of organic dye degradation, extensive efforts have been devoted to regulating interfacial structures and material systems to systematically elucidate how material design strategies influence the efficiency and stability of CEC [74–76]. As interfacial electron transfer constitutes the key step in this process, modulation of the surface electronic structure is widely recognized as a direct determinant of ROS generation [16,56,77,78]. Among various approaches, surface fluorination has emerged as a general and effective interfacial regulation strategy, as it markedly enhances electron affinity and CE strength. For example, Gan et al. [44] reported a CEC system employing surface-fluorinated silicon powders (F-Si) as an alternative to conventional fluoropolymer dielectrics, in which a mild self-assembly fluorination strategy substantially strengthened solid–liquid interfacial electron transfer, enabling efficient ultrasonic degradation of methyl orange and phenol. Compared with unmodified silicon, F-Si exhibited an approximately 30-fold enhancement in methyl orange degradation efficiency, and its phenol degradation performance was about four times higher than that of size-matched FEP powders. Similarly, introducing fluorinated functional groups (e.g., 1 H, 1 H, 2 H, 2H-perfluorodecyltriethoxysilane (FDTES)) onto silicon or silica surfaces significantly accelerated methyl orange degradation without relying on bulk fluoropolymer matrices, underscoring surface fluorination as an effective means of tuning CE activity [54,61,79]. In addition, two-dimensional inorganic fluorinated materials have also been explored for CEC-driven dye degradation. Fluorinated graphite, as a representative example, maintains stable catalytic activity even at elevated temperatures, achieving efficient methyl orange removal within several hours

while exhibiting good cycling stability [60]. Meanwhile, porous and framework materials have been introduced to improve interfacial accessibility and tailor the reaction microenvironment. In zeolitic systems, immobilizing small amounts of PTFE onto porous supports allows PTFE to remain the primary electron acceptor, while the pore structure and surface hydrophilicity of the zeolite enhance dispersion and interfacial contact in aqueous media, thereby accelerating azo-dye degradation (Fig. 2g) [75]. Similarly, metal-organic frameworks (MOFs), owing to their tunable ligand structures and ordered pore architectures, have been employed to regulate triboelectric properties and interfacial charge distribution, enabling efficient removal of organic dyes [76]. Collectively, these studies indicate that porous architectures mainly function to amplify interfacial interactions and promote reaction synergy in CEC. In some cases, magnetic nanoparticles have been incorporated to facilitate rapid catalyst separation and recovery, with their primary contribution lying in improved operational convenience and recyclability rather than changes in the intrinsic reaction mechanism [61].

Recent advances in CEC have increasingly focused on the role of interfacial electric fields in governing electron transfer, radical generation, and reaction selectivity at solid-liquid interfaces [34,75]. Polarized PTFE electrets, prepared via high-voltage corona polarization, achieve charge preservation for a long time, leading to markedly enhanced ROS generation and accelerated MO degradation with excellent cycling stability [46]. In addition, metal-dielectric hybrid architectures provide an additional route to tailoring interfacial electronic environments [33,34]. For example, polymer/metal Janus and multilayer systems demonstrate that metal coatings can modulate electron injection pathways by altering surface electronic states, thereby enhancing dye degradation kinetics compared with pristine dielectrics (Fig. 2h) [34]. Systematic studies further reveal that different metal configurations distinctly influence ROS yields and degradation efficiencies, underscoring the sensitivity of CEC to interfacial electronic structure (Fig. 2i) [33]. Collectively, these findings highlight interfacial electric fields as a central factor coupling charge transfer, radical generation, and reaction pathways, offering a unifying framework for the rational design of CEC systems.

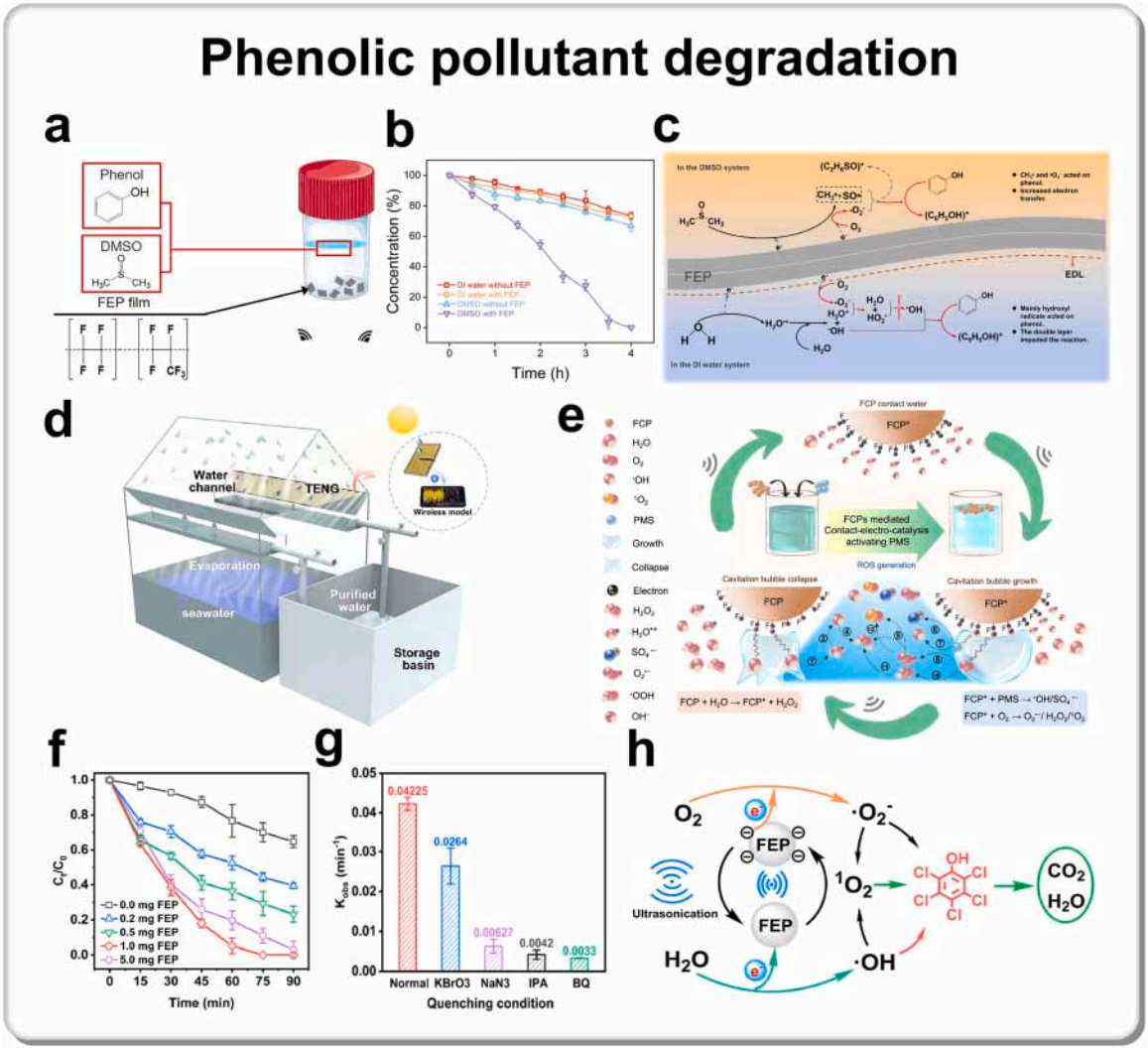

Fig. 3. Applications of CEC: organic pollutant degradation (phenolic pollutant degradation). (a) Schematic of the experimental setup and protocol for the degradation of phenol. (b) UV-Vis spectra of phenol degradation with different conditions. (c) Mechanism of CEC in different solvents. Reproduced with permission [32]. Copyright 2024, American Chemical Society. (d) Schematic illustration of the application concept for a solar-driven droplet-based system for phenol degradation. Reproduced with permission [82]. Copyright 2025, Wiley. (e) The schematic of fluorocarbon polymers (FCPs)-mediated CEC activating peroxymonosulfate (PMS) for phenolic pollutant degradation. Reproduced with permission [39]. Copyright 2025, Wiley. (f) Effect of FEP dosage on degradation of pentachlorophenol (PCP). (g) Comparison of the reaction rate constant for PCP removal by different scavengers. (h) Possible mechanism of degradation of PCP in CEC system. Reproduced with permission [62]. Copyright 2024, American Chemical Society.

3.1.2. Phenolic pollutant degradation

Phenolic pollutants constitute a widespread class of organic pollutants in industrial wastewater and polluted aquatic environments, with representative examples including phenol, halogenated phenols, and bisphenol A [39,40,62,64]. These pollutants are typically characterized by high chemical stability and pronounced biological toxicity [32,63]. The halogenated phenols and BPA further exhibit strong environmental persistence and potential endocrine-disrupting effects, rendering them difficult to remove effectively by conventional biological treatments or traditional oxidative processes [62,64]. Consequently, there is a pressing need for alternative treatment strategies capable of achieving efficient degradation under mild conditions while minimizing the formation of highly toxic intermediates [80,81]. In recent years, growing evidence has demonstrated that CEC enables the in situ generation of multiple ROS through interfacial electron transfer, thereby offering a distinct reaction pathway for phenolic pollutant degradation that differs fundamentally from conventional advanced oxidation processes [32,64,82].

In the structurally simplest phenol system, early studies first established the fundamental applicability of CEC to phenolic pollutants. Liu et al. [32] demonstrated that CE between dielectric materials and liquid phase induces interfacial electron transfer, leading to the generation of •OH, $\bullet O_2^-$, and $\bullet CH_3$, which collectively drive the continuous oxidation and mineralization of phenol (Fig. 3a). Compared with aqueous systems, aprotic organic solvents provide a more favorable environment for interfacial charge regulation in CEC and enable markedly faster reaction kinetics (Fig. 3b). In water, interfacial electron transfer is inherently coupled with solvent ionization and ion accumulation, readily forming a compact EDL at the solid-liquid interface that progressively screens further charge transfer and limits reaction sustainability. By contrast, organic media such as DMSO, characterized by low ionic strength and weak self-dissociation, suppress the formation of a dense EDL, allowing triboelectrically generated electrons to accumulate at the interface and continuously participate in subsequent reactions (Fig. 3c). This work identifies organic systems as a powerful platform for probing the intrinsic mechanisms of CEC and for extending its reaction scope, laying a critical foundation for the efficient and controllable degradation of increasingly complex phenolic pollutants, including halogenated phenols and bisphenol A. In addition, subsequent studies further introduced light fields in synergy with CEC to enhance phenol degradation efficiency (Fig. 3d). The photo-CE coupled system promotes the CE-induced interfacial electron-transfer process and facilitates the separation of photogenerated electron-hole pairs, increasing the overall generation rate of ROS [82]. Compared with standalone CE-driven or conventional photocatalytic systems, the synergistic strategy exhibits markedly improved degradation kinetics for phenol. These results highlight that CEC can operate in a complementary rather than competitive manner with external fields, offering a flexible route to promote interfacial charge transfer and modulate reaction efficiency.

Furthermore, CEC has been extended to the degradation of bisphenol A, a molecule with higher structural complexity [39,41]. The degradation process was dominant with $^1O_2$ pathway, accompanied by radical pathways (•OH, $SO_4^{\bullet-}$, and $\bullet O_2^-$), avoiding limitations associated with single-pathway reactions (Fig. 3e) [39]. In addition, for halogenated phenols, which exhibit greater structural complexity and higher toxicity, CEC displays reaction characteristics distinct from those of conventional oxidative processes [62,64]. In chlorophenol and pentachlorophenol (PCP) systems, studies have shown that CEC can not only induce oxidative cleavage of the benzene ring but also concurrently trigger reductive dichlorination [62]. Through multistep reaction pathways involving ROS, chlorine substituents are progressively removed, thereby significantly reducing the toxicity of reaction intermediates [64]. Notably, in the PCP system, increasing the amount of the dielectric material FEP enhances interfacial charge transfer and promotes degradation, but excessive FEP dosage leads to ultrasonic attenuation, which in turn suppresses PCP degradation (Fig. 3f). Quenching experiments further confirm that PCP degradation proceeds via the synergistic involvement of multiple ROS, including •OH, $\bullet O_2^-$, and $^1O_2$, collectively driving direct dechlorination, hydroxylation dechlorination, oxidation, and polymerization (Fig. 3g). This concerted reaction pathway effectively avoids the accumulation of highly toxic chlorinated intermediates, highlighting the safety advantages of CEC in the treatment of highly halogenated phenolic pollutants (Fig. 3h).

Overall, studies on phenol, halogenated phenols, and bisphenol A collectively demonstrate that CEC can generate multiple reactive species via interfacial electron transfer and drive efficient degradation of phenolic pollutants under mild conditions [40]. In contrast to conventional advanced oxidation technologies, this approach not only enables benzene ring oxidation but can also, under specific conditions, promote concurrent processes such as dehalogenation, thereby effectively reducing the toxicity of reaction intermediates [32,62]. The distinct reaction pathways observed for different phenolic pollutants in CEC further highlight the adaptability and versatility of this approach for treating structurally complex and toxic organic pollutants, providing important experimental evidence for its potential application in practical water treatment systems.

3.1.3. Antibiotics degradation

Antibiotics are a representative class of trace organic contaminants that are ubiquitously detected in municipal wastewater treatment plant effluents, surface waters, and groundwater systems [83,84]. Their long-term persistence at low concentrations not only poses potential ecotoxicological risks to aquatic environments but is also widely recognized as a key environmental driver for the dissemination of antibiotic resistance [85,86]. Typical examples include sulfamethoxazole (SMX), ciprofloxacin (CIP), tetracycline (TC), and levofloxacin (LEV) [83]. These pollutions generally feature structurally complex and multifunctional molecular architectures and exhibit high chemical stability in aqueous environments, rendering them difficult to remove efficiently and sustainably using conventional biological treatments or standard advanced oxidation processes [87,88]. Against this backdrop, CEC, which enables the direct transformation of antibiotic molecules under mild conditions without reliance on electrodes or externally applied energy fields, has emerged as a promising and distinctive strategy for antibiotic degradation [65–67,89].

From an engineering feasibility perspective, initial studies have demonstrated the effectiveness of CEC for antibiotic degradation in real and compositionally complex water matrices [65]. Using reusable PTFE dielectric particles as the CE material, Cao et al. [65] systematically investigated the removal of SMX, CIP, and TC in secondary effluents from municipal wastewater treatment plants (Fig. 4a). In the absence of externally added oxidants, the CEC system achieved degradation efficiencies of approximately 50% for SMX, 80% for CIP, and 90% for TC within 90 min (Fig. 4b), indicating that ROS generated via interfacial electron transfer remain effective across structurally diverse antibiotics even under realistic water conditions (Fig. 4c). Furthermore, the construction of polyvinylidene fluoride (PVDF) electrospinning nanofiber membranes enabled efficient recovery and reuse of PTFE particles, providing critical support for the practical implementation and scalability of CEC in antibiotic treatment applications. Building on these findings, subsequent studies have progressively coupled CEC with oxidants such as peroxymonosulfate (PMS) to broaden reaction pathways and further enhance degradation efficiency [89]. Using TC as a model compound, Liu et al. [89] employed modified ethylene-propylene-diene-monomer (EPDM) rubber as the CE material, enabling effective PMS activation through CE-induced interfacial charge transfer. Under near-neutral conditions, more than 90% TC removal was achieved within 30 min. Mechanistic investigations revealed that the degradation process is governed by the synergistic involvement of multiple reactive species, predominantly $^1O_2$ and $SO_4^{\bullet-}$, and intermediate analysis combined with toxicity assessment confirmed a substantial reduction in the ecological toxicity of transformation products. This

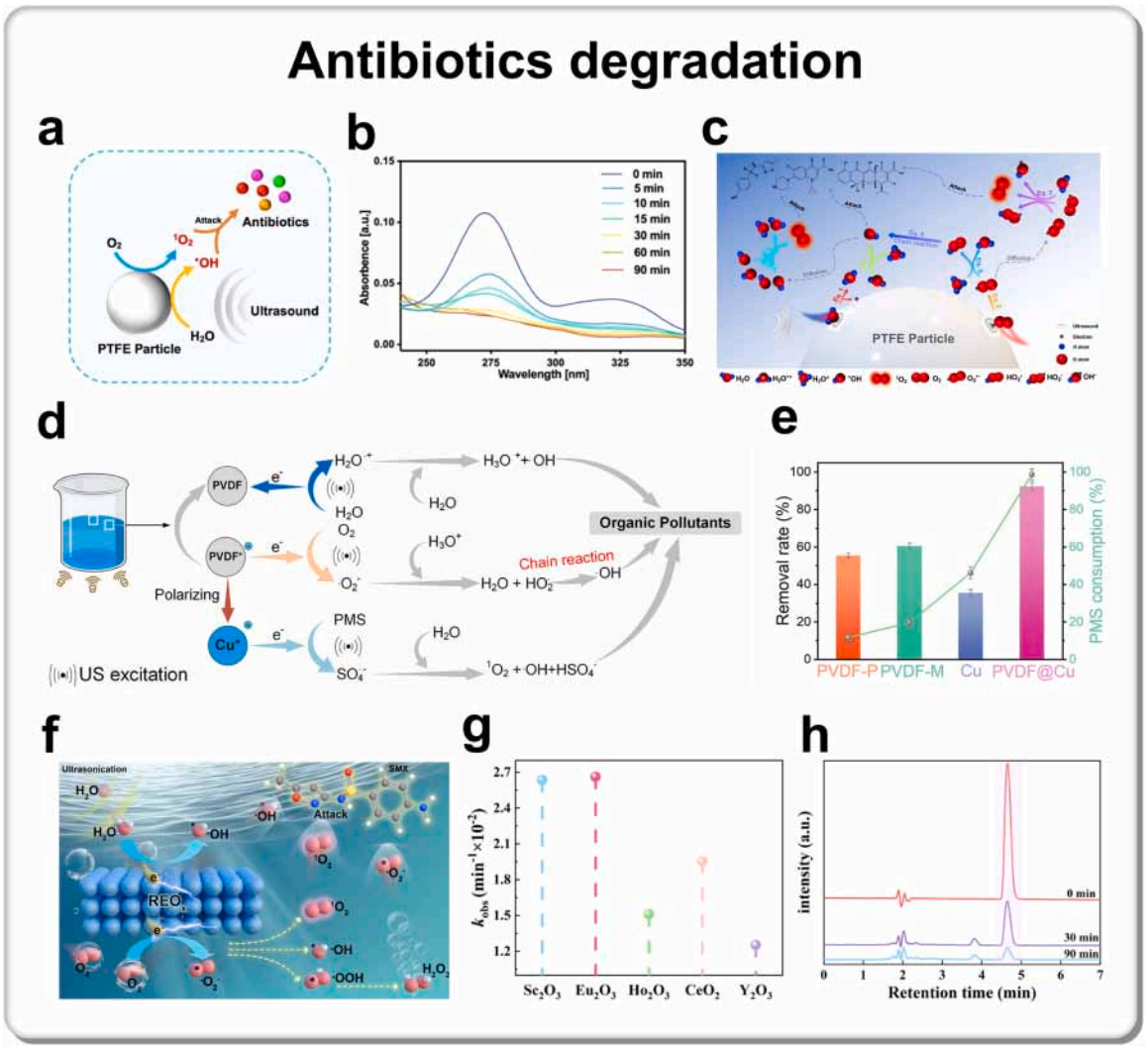

Fig. 4. Applications of CEC: organic pollutant degradation (antibiotics degradation). (a) Schematic of antibiotic degradation via CEC. (b) UV-Vis spectra of the solutions obtained after an ultrasound of 0–90 min for a ciprofloxacin (CIP) solution in the presence of PTFE particles. (c) Mechanism of CEC in antibiotic degradation. Reproduced with permission [65]. Copyright 2024, Elsevier. (d) Proposed mechanism for levofloxacin (LEV) degradation by CEC generated ROS. (e) PMS consumption in different systems. Reproduced with permission [66]. Copyright 2025, Elsevier. (f) Schematic of antibiotic degradation via rare-earth oxides (REO_x). (g) Observed rate constants (k_{obs}) of different materials. (h) High performance liquid chromatography (HPLC) monitoring of SMX degradation (0, 30, 90 min). Reproduced with permission [62]. Copyright 2024, American Chemical Society.

work demonstrates that CEC not only accelerates antibiotic degradation but also offers a means to modulate reaction selectivity and environmental safety through controlled coupling with oxidant activation.

Further studies have shifted the focus from whether degradation can be achieved to how interfacial structures can be precisely engineered to regulate electron transfer processes. By constructing a Janus-structured PVDF@Cu composite, Wang et al. [66] integrated the charge accumulation capability of β-phase-enriched PVDF with the electronic responsiveness of a Cu interface, markedly enhancing CE-induced PMS activation in the LEV degradation system (Fig. 4d). Experimental results showed that, compared with pristine PVDF, the PVDF@Cu system exhibited 1.8-fold improvement in LEV degradation efficiency and an 8.6-fold increase in PMS utilization (Fig. 4e). Notably, this work further introduced electrical current signals as real-time feedback parameters for reaction progress, demonstrating the potential of CEC to achieve coupled reaction–monitoring functionalities during antibiotic degradation. Beyond polymeric dielectric materials, antibiotic degradation studies have been extended to more chemically robust inorganic dielectrics (Fig. 4f) [67]. Using rare-earth oxides as representative examples, Eu_2O_3 was found to exhibit pronounced activity toward SMX degradation in CEC systems, achieving removal efficiencies exceeding 90% within 90 min (Fig. 4g-h). In this system, $\bullet O_2^-$ was identified as the dominant reactive species, while H_2O_2 was concurrently generated during the reaction, highlighting the potential of CEC to couple antibiotic degradation with functional chemical production, providing mechanistic insight and new guidance for the rational design of dielectric materials for antibiotic degradation applications.

Overall, studies centered on representative antibiotics such as SMX, CIP, TC, and LEV demonstrate that CEC can efficiently degrade structurally diverse antibiotic molecules under mild conditions without the need for electrodes or externally applied fields, by driving the in situ generation of multiple ROS via interfacial electron transfer [67]. Through coupling with oxidants, interfacial structure engineering, and expansion of material systems, CEC has shown continuously improving performance in terms of degradation efficiency, reaction selectivity, and engineering applicability [66,89]. These advances not only provide alternative strategies for antibiotic pollution control but also establish an important foundation for extending CEC to the treatment of more complex classes of micropollutants.

3.1.4. Other organic pollutant degradation

In these studies, CEC has been extensively applied to the degradation of typical aqueous organic pollutions, including dyes, phenolic pollutions and antibiotics, demonstrating a distinctive capability to generate ROS without the need for external electrodes or applied bias [7,16]. Beyond these conventional targets, CEC has also been increasingly explored for the transformation of other challenging organic systems, such as per- and polyfluoroalkyl substances (PFAS), potassium butylxanthate (PBX), bromophenol blue (BPB), and solid organic biomass exemplified by lignocellulosic straw [35,68,70,90]. Owing to their high bond dissociation energies and structural complexity, these substrates are generally refractory to efficient conversion by traditional advanced oxidation processes, highlighting the significance of CEC as an alternative, interface-driven reaction paradigm.

In the context of PFAS remediation, the US/PTFE system provided the first experimental evidence that, under low-frequency ultrasound, the polymer-water interface can establish an extremely strong localized electric field, which markedly weakens the stability of otherwise inert C-F bonds and, in concert with ROS such as •OH, $\bullet O_2^-$, enables efficient defluorination and mineralization (Fig. 5a-b) [36]. Moreover, building on this concept, Wang et al. [35] developed an "island-sea" Cu-N/C@PVDF hybrid architecture (Fig. 5c), in which a β-phase-enriched PVDF matrix constructs a highly polarized interface, while Cu-N_4 single-atom sites serve as centers for directional electron utilization, leading to substantially enhanced PFAS degradation, defluorination efficiency and operational stability (Fig. 5d-e). Collectively, these works advance CEC from a paradigm primarily reliant on strong interfacial electric fields to one in which interfacial electron dynamics can be rationally engineered, offering a general materials strategy for the selective activation of inert C-F bonds. In the extended application to complex organic systems, CEC demonstrates broad versatility through the synergistic coupling of materials engineering and reaction-scenario design. For example, Ye et al. [68] developed a fluorinated magnetic mesoporous material (Fluorine-AFS) that markedly amplifies CEC, delivering nearly three orders of magnitude enhancement in PBX degradation kinetics through the combined effects of surface fluorination, mesoporous nano-confinement and improved aqueous dispersibility. The material enables near-complete pollutant removal with

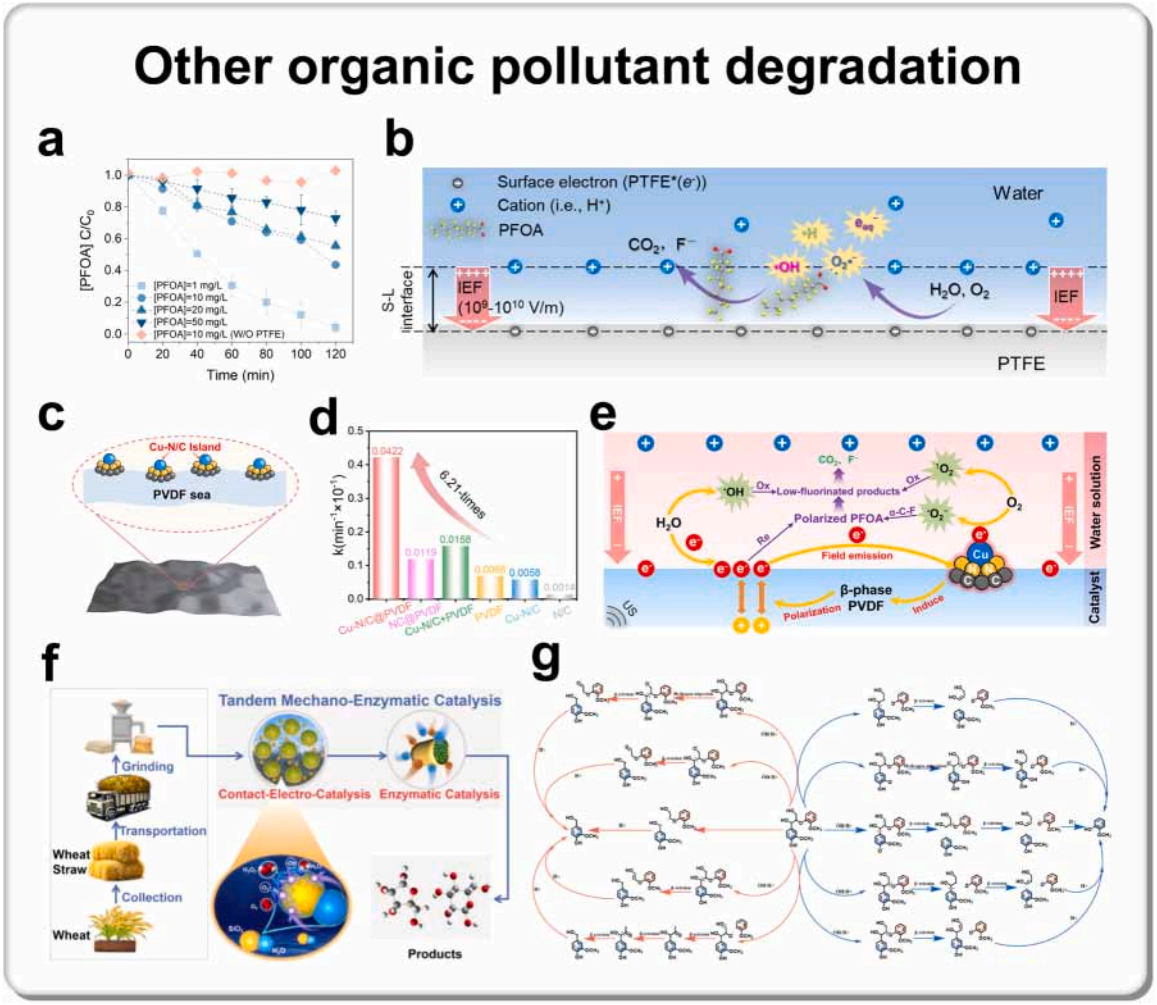

Fig. 5. Applications of CEC: organic pollutant degradation (other organic pollutant degradation). (a) Schematic of antibiotic degradation via CEC. The effect of perfluorooctanoic acid (PFOA) concentration on US/PTFE system. (b) Diagram of PFOA degradation process on PTFE-water interface. Reproduced with permission [36]. Copyright 2024, Wiley. (c) Structure diagram of Cu-N/C@PVDF. (d) The corresponding degradation kinetic rate constants for PFOA removal of the different system. (e) Proposed mechanism of β-phase-mediated IEF-driven PFAS defluorination (O_x: oxidation, Re: reduction). I. US induces piezoelectric polarization in the β-phase PVDF; II. The resulting IEF drives directional electron emission from the matrix to Cu-N_4 islands; III. Accumulated electrons activate adsorbed O_2 into ROS while simultaneously polarizing C-F bonds; IV. Cooperative attack by ROS and electrons triggers cascade defluorination and mineralization to CO_2 and F^-. Reproduced with permission [35]. Copyright 2025, Wiley. (f) schematic of the tandem mechano-enzymatic catalysis for pristine wheat straw. (g) Proposed reaction pathways of the lignocellulosic biomass by the tandem mechano-enzymatic catalysis. Bond fission, hydrogen abstraction, intramolecular H-migration, and β-scission reactions are included. Reproduced with permission [62]. Copyright 2025, American Chemical Society.

high durability and recyclability at the pilot scale, while producing bio-safe effluents compatible with hybrid wastewater treatment systems. In addition, Li et al. [70] extend CEC beyond aqueous-phase pollutant oxidation to the treatment of solid organic matrices, enabling the effective pretreatment of lignocellulosic biomass such as straw under low energy input (Fig. 5f). Under ambient conditions, this system achieves more than 80% degradation of wheat straw within 4 h, substantially disrupting its compact structure; compared with

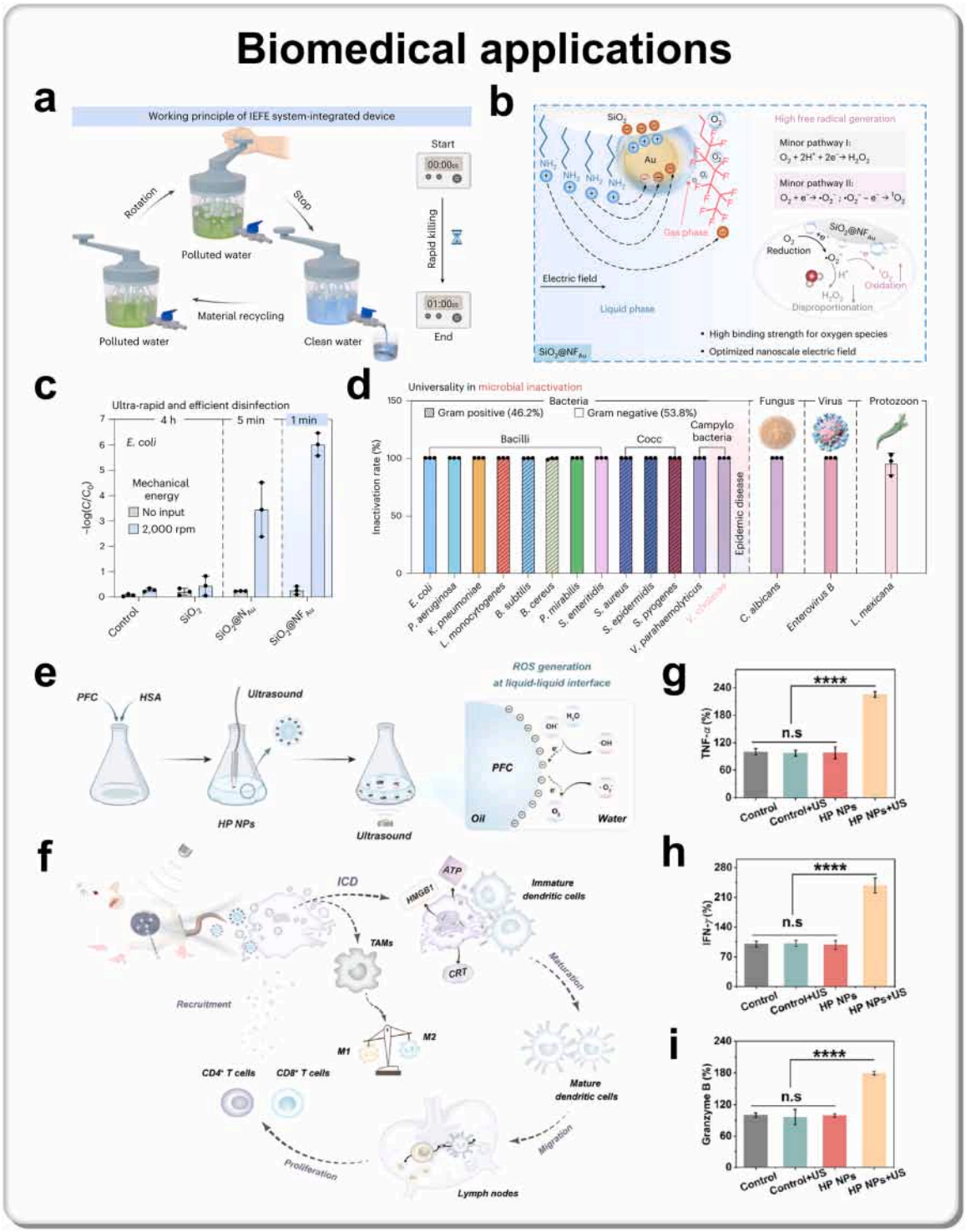

Fig. 6. Applications of CEC: Biomedical applications. (a) Schematic of the working principles of the system. (b) Design of the system with an enhanced nanoscale electric field. (c) Disinfection performance of SiO_2@NFAu and comparative samples with and without vortexing. (d) Rapid inactivation of various microorganisms, including bacteria spanning bacilli (rod-shaped), cocci (spherical; Cocc) and campyliform/curved forms (Campylo; Campylobacter-like), fungi, viruses and protozoa, by SiO_2@NFAu within 5 min. Reproduced with permission [93]. Copyright 2025, Springer Nature. (e) Schematic illustration of the preparation of human serum albumin (HAS)-modified perfluorotributylamine (PFTBA) nanoemulsions (HP NPs), ROS Generation in liquid-liquid CE. (f) ROS-induced immunogenic cell death (ICD)-mediated immune recruitment and adaptive immune response. Percentage of cytokine (g) TNF-α, (h) IFN-γ, and (i) granzyme B content from tumors of each group. Reproduced with permission [96]. Copyright 2024, American Chemical Society.

ultrasound alone, the CEC process enhances the enzymatic conversion efficiencies of cellulose and hemicellulose by 35.8% and 78.1%, respectively, while markedly reducing crystallinity (Fig. 5g).

Collectively, these studies indicate that CEC is evolving from its initial application in the degradation of relatively simple aqueous organic pollutants toward more challenging targets, including PFAS with strong covalent bonds, structurally complex industrial organic contaminants, and even solid biomass systems. Through the rational construction of interfacial electric fields, the design of electron-transfer pathways, and the engineering of material architectures, CEC continues to extend the boundaries of conventional advanced oxidation technologies in terms of reaction depth, energy efficiency, and applicability. These advances suggest that CEC has the potential to emerge as a general interfacial reaction platform for diverse organic pollutant remediation and organic resource transformation, providing new theoretical foundations and technological routes for low-energy-input and sustainable environmental and biomass processing.

3.2. Biomedical applications

CEC exploits CE and interfacial electron transfer at solid-liquid or liquid-liquid interfaces to generate ROS without the addition of external chemical reagents, establishing a physically triggered, interface-mediated route to biological effects for disinfection and antitumor therapy [91–94]. In contrast to conventional oxidant dosing or electrolytic processes, these systems typically rely on ultrasound or mechanical agitation to intensify contact–separation events, enabling mobile and distributed operation while maintaining effectiveness in complex aqueous environments and heterogeneous biological microenvironments [93,95]. Recent studies along this line can be broadly classified into two application paradigms: rapid, broad-spectrum disinfection for public health protection [91,93–95], and ROS-driven antitumor therapies that further engage immune activation within the antitumor microenvironment [92,96,97].

First, for disinfection and the control of biological hazards in aquatic environments, Wei et al. [95] demonstrated that low-frequency ultrasound-enhanced water–PTFE CE can effectively inactivate Microcystis aeruginosa while simultaneously reducing algal toxins. Within 5 h, an algal cell removal efficiency of 60.19% was achieved ($k = 0.1591\ h^{-1}$), and the degradation of microcystin-LR (MC-LR) reached 97.2%, markedly outperforming ultrasound treatment alone, thereby highlighting the advantage of ROS generated via CEC for complex biological particulate systems. Building on this concept, Chen et al. [93] further engineered the interfacial reaction into a hand-powered interfacial electric-field-enhanced (IEFE) disinfection system (Fig. 6a), in which fluorinated SiO_2-supported Au nanoparticles (SiO_2@NFAu) were employed to amplify ROS generation (Fig. 6b). This system enabled 99.9999% inactivation of Vibrio cholerae within 1 min, with a kinetic rate constant of 15.06 min^{-1}, representing a 6375-fold enhancement compared with pristine SiO_2 (0.0024 min^{-1}) (Fig. 6c). Given the diversity of pathogens potentially contaminating water sources, including bacteria, fungi, viruses and parasites, 16 representative highly infectious microorganisms were selected for evaluation; the results showed that more than 95% of the tested microbes were inactivated within 5 min (Fig. 6d). This work has the potential to markedly advance global water, sanitation and hygiene (WASH) initiatives and support the World Health Organization's Global Roadmap to 2030.

In antitumor therapy, researchers have approached the problem from both solid–liquid and liquid-liquid interfaces, collectively demonstrating the feasibility and tunability of an "interfacial CE, ROS generation, antitumor cell apoptosis and immune activation" paradigm. For instance, Zhang et al. [97] employed SiO_2 microspheres in combination with ultrasound to amplify ROS signals by approximately 13.8-fold at the cellular level, increasing the apoptosis rate from 14.2% to 37.8%, while simultaneously enhancing the proportion of mature dendritic cells ($CD80^+CD86^+$) by 4.5-fold relative to controls. This study provides a multimodal non-drug anticancer therapy targeting the complex tumor environment with translational potential. In parallel, Li et al. [96] constructed a liquid–liquid interfacial platform using human serum albumin (HSA)-modified perfluorotributylamine (PFTBA) nanoemulsions (HP NPs) (Fig. 6e), where 5 min of ultrasound irradiation increased cellular ROS signals to 3.8 times those at 0 min and elevated the fraction of mature dendritic cells by 3.2-fold. The activated T cells further secreted antitumor necrosis tumor necrosis factor (TNF)-α, interferon (IFN)-γ, granzyme B, and perforin, inducing antitumor cell death, triggering apoptotic signaling pathways and eliciting a robust antitumor immune response in vivo (Fig. 6f-i). These results highlight and underscore that liquid-liquid interfaces can also serve as deep-penetrating, low-toxicity ROS generators. Moreover, Li et al. [92] reinforced the mechanistic framework of therapeutic CEC by identifying an additional reaction pathway beyond WOR/ORR, whereby the Perfluorocarbon (PFC)-water interface promotes the reduction of H_2O_2 to generate •OH radicals; this route can be further amplified by introducing glucose oxidase to elevate intratumoural H_2O_2 levels. In vivo treatment using PFC nanoemulsions (2.5 mg kg^{-1}) in combination with GOD (75 mg kg^{-1}) and ultrasound irradiation (3 kHz, 1 W cm^{-2}, 50% duty cycle, 10 min) resulted in pronounced antitumor growth inhibition without noticeable body-weight loss, indicating a favorable safety window and promising scalability.

Overall, this section delineates a clear dual-application trajectory for CEC. On one hand, interfacial generated ROS enable rapid, broad-spectrum disinfection and biological hazard control, exemplifying the translation from mechanistic understanding to device-level implementation [92,93]. On the other hand, ultrasound-triggered interfacial ROS act as therapeutic effectors that further engage antitumor immunity, while the identification of an additional H_2O_2 reduction to •OH pathway expands the accessible reaction space at the mechanistic level [92]. Collectively, these studies point to several critical future breakthroughs, including the quantitative regulation of ROS identity and flux in complex matrices and antitumor microenvironments, the definition of boundaries for side reactions and collateral tissue damage, and the systematic integration with portable disinfection units or immunotherapeutic combinations, advancing CE-driven disinfection and therapy towards more verifiable and scalable public health and biomedical technology platforms.

3.3. Direct synthesis of H_2O_2

The direct synthesis of H_2O_2 has traditionally relied on centralized infrastructures and specialized electrochemical or chemical processes [98,99]. In recent years, however, a class of CEC pathways driven by solid-liquid interfacial charge transfer and ROS generation have emerged as an alternative route for producing H_2O_2 under ambient conditions without external power input [100–103]. Early observations in microfluidic systems revealed that flowing water in contact with solid surfaces can generate quantifiable amounts of H_2O_2 on the timescale of seconds (for example, reaching a maximum within ~10 s and up to 1.9 mg L^{-1} in microchips), suggesting that the water–solid interface itself can function as a potential "distributed hydrogen peroxide generator" [100]. Building on this concept, strategies that increase interfacial contact frequency, enhance charge transfer and radical coupling, and incorporate materials structural engineering have enabled this interfacial phenomenon to evolve into a sustainable and engineering-scalable platform for the direct synthesis of H_2O_2.

From both mechanistic and implementation perspectives, these studies can be distilled into four progressively scalable strategies. First, quantification and regulation of interfacial origins were established: Chen et al. [100] demonstrated that solid–liquid CE induced by liquid flow in microfluidic chips can directly generate H_2O_2, and revealed that the decline in H_2O_2 yield with increasing ionic strength arises from EDL screening in aqueous solutions, providing fundamental design principles for subsequent materials and reactor architectures. Second, mechanical

stimulation to amplify CE processes was introduced: Wang et al. [104] reported a simple "PTFE stir bar + ultrasound" system (Fig. 7a) that achieves an H_2O_2 generation rate of 256.6 μM h^{-1} in the absence of catalysts and sacrificial agents, demonstrating that high-throughput production is accessible even in minimalistic setups (Fig. 7b-c). Building on this concept, Zhao et al. [103] developed a PTFE powder-water solid–liquid CE reactor capable of directly producing H_2O_2 under mild conditions (Fig. 7d), and clarified that the process proceeds through sequential water oxidation reaction (WOR) and oxygen reduction reaction (ORR) steps (Fig. 7e), reaching rates up to 313 μM h^{-1}. In parallel, Berbille et al. [102] showed that, mediated by the hydrogen bond network of water, ROS can migrate and couple via a Grotthuss mechanism with kinetics as high as 58.87 mM g^{-1} h^{-1}. Third, materials engineering coupled with external fields to enhance charge-carrier utilization was exemplified by resorcinol formalde resin/-polytetrafluoroehtylene (RF/PTFE) composites, where interfacial electric field promotes photogenerated charge separation, enabling synergistic visible-light and ultrasonic H_2O_2 production at 56.5 μmol h^{-1} and offering a broadly transferable paradigm based on "material hybridization + interfacial field regulation" [105]. Finally, with an eye toward practical implementation, flow-based contact electrochemistry systems were proposed to overcome mass-transfer and contact-efficiency limitations imposed by PTFE hydrophobicity in batch reactors [106]. Continuous flow packed column reactors (12 μm PTFE particles, 35 mm column length, 0.1–1.0 mL min^{-1} flow rates) upgrade the reaction interface from intermittent contact to continuous renewal (Fig. 7f), achieving maximum productivities of 10.7 mM h^{-1}, claimed to be a 34-fold enhancement over batch operation, and marking a transition from mechanistic proof-of-concept toward integrable process units.

Overall, these studies collectively delineate a clear technological evolution of direct H_2O_2 synthesis, progressing from visualized evidence of spontaneous interfacial generation to mechanical stirring- or ultrasound-enhanced systems, material composite with external-field synergy, and ultimately continuous-flow amplification. A central consensus emerging from this body of work is that solid–liquid interfacial charge generation and electron injection can trigger aqueous redox processes to produce H_2O_2 under mild conditions, while the achievable yields are strongly modulated by interfacial area, contact frequency, solution ionic strength and pH, as well as by materials structure and their coupling with external fields [100,102]. Future breakthroughs are expected to focus on maintaining high efficiency and selectivity in complex water matrices, suppressing parasitic reactions and peroxide decomposition, and tightly integrating continuous reactors with downstream oxidation, disinfection, or chemical synthesis units. Together, these advances are poised to transform CEC H_2O_2 production into a scalable, distributed, and green manufacturing platform for oxidants.

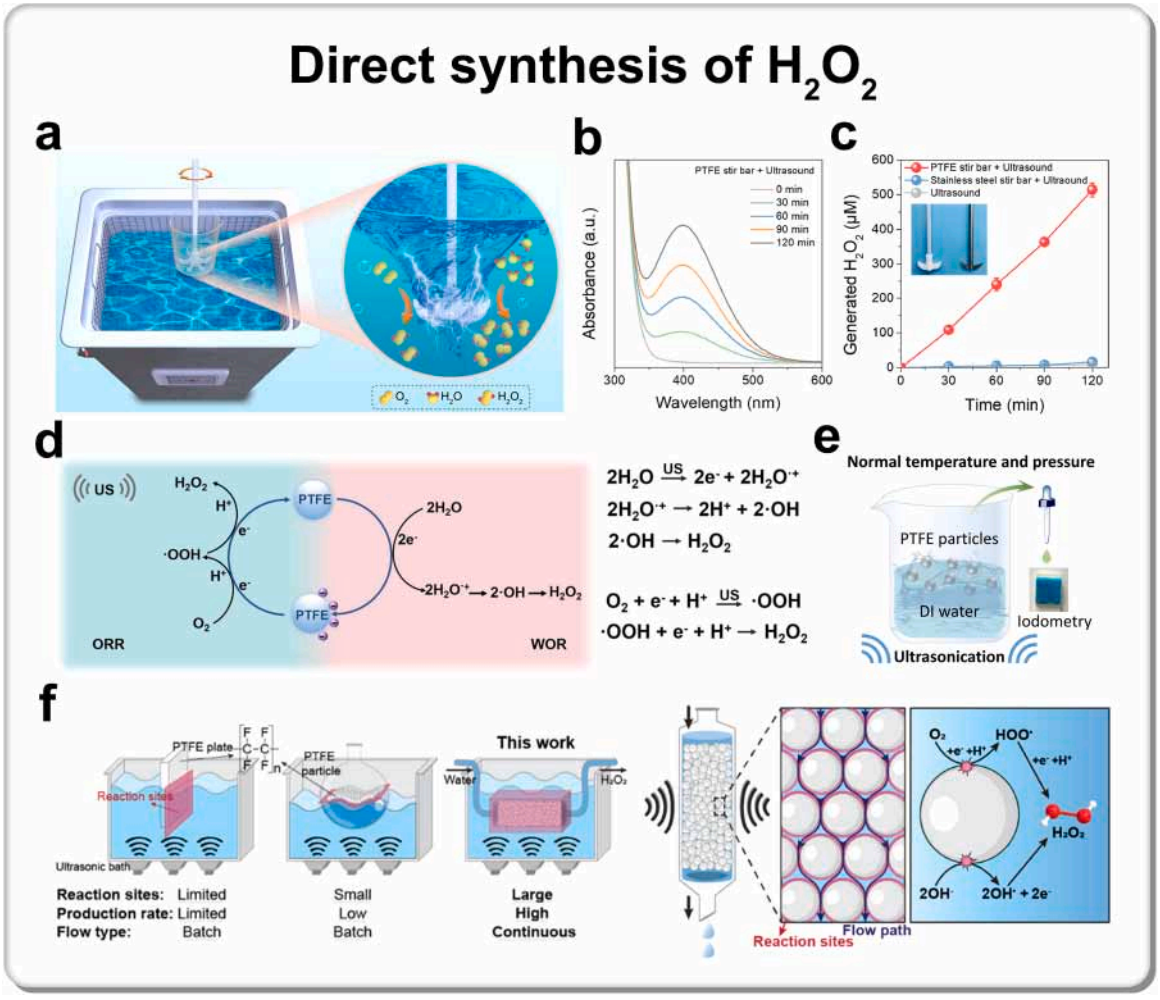

Fig. 7. Applications of CEC: Direct synthesis of H_2O_2. (a) Schematic of the experimental setup for H_2O_2 generation. (b) Absorption spectrum of e potassium titanium oxalate (PTO) in the reaction solution of the "PTFE stir bar + ultrasound" system. (c) Comparison of H_2O_2 generation using PTFE and stainless steel stir bars. Reproduced with permission [104]. Copyright 2024, The Royal Society of Chemistry. (d) Proposed reaction mechanism of contact-electro-catalysis for H_2O_2 generation. (e) Schematic representation of the experimental setup and overall reaction. Reproduced with permission [103]. Copyright 2024, Wiley. (f) Schematic illustration of batch and continuous flow contact electrocatalysis. Reproduced with permission [106]. Copyright 2025, American Chemical Society.

3.4. Activation of gas molecules

The inertness of small gas molecules such as N_2, CO_2, and CH_4, arising from strong covalent bonds and substantial kinetic barriers, renders conventional processes heavily dependent on high temperatures and pressures, external electrical inputs, and costly metal-based catalysts [12,107–111]. In this context, emerging CEC strategies exploit CE at gas-liquid-solid three-phase interfaces to drive interfacial charge transfer, generating ROS and key reaction intermediates that enable the activation and directional transformation of gas molecules under mild conditions [112,113].

In nitrogen fixation, Li et al. [114] first proposed a continuous ammonia synthesis strategy driven by CE at FEP-water interfaces, in which ultrasonication promotes repeated contact-separation events to sustain interfacial charge transfer and reaction progression under ambient conditions (Fig. 8a). During 8 h of continuous operation, the system delivered an average ammonia production rate of 420 μM h^{-1} g^{-1} (Fig. 8b-c). In parallel, Huang et al. [113] demonstrated an direct air/water-to- nitrate route with an average nitrate formation rate of 40.73 μM h^{-1} in air gas atmosphere, which validates the feasibility of using atmospheric nitrogen as the feedstock and provides a new reaction paradigm and conceptual framework for distributed nitric acid production under mild conditions. Subsequently, Wu et al. [112] reported a dual-pathway nitrogen fixation system that simultaneously channels N_2 toward nitrate and ammonium, with parallel formation rates of 330.65 and 68.16 μM h^{-1}, respectively, highlighting that oxidative and reductive nitrogen fixation can coexist on a single CEC platform through interfacial charge and ROS regulation, providing a foundation for selective control and coupled separation. Building on these advances, Shi et al. [108] further coupled CEC with photoexcitation, achieving an ammonia production rate of 133.6 μmol g^{-1} h^{-1}, offering a reproducible paradigm for synergistic external-field modulation and dielectric interfacial charge engineering.

In the carbon cycle, Wang et al. [107] highlighted the pivotal role of interfacial CO_2 enrichment in enabling the capture and activation of low-concentration CO_2, including CO_2 at atmospheric levels. By constructing a system based on electrospun PVDF loaded with single Cu atoms-anchored polymeric carbon nitride (Cu-PCN) materials and quaternized cellulose nanofibers (CNF) nanofibers, CO_2 was effectively concentrated at the interface, resulting in the highly selective formation of CO (Fig. 8d). The CO production rate of 33.0 μmol g^{-1} h^{-1} was achieved with a corresponding Faradaic efficiency of 96.24%, underscoring the potential of CEC platforms to integrate CO_2 capture, activation, and conversion within a single framework (Fig. 8e). Moreover, using a similar architecture, Wang et al. [115] also realized CO_2 reduction with product distributions dominated by CO and ethylene, for

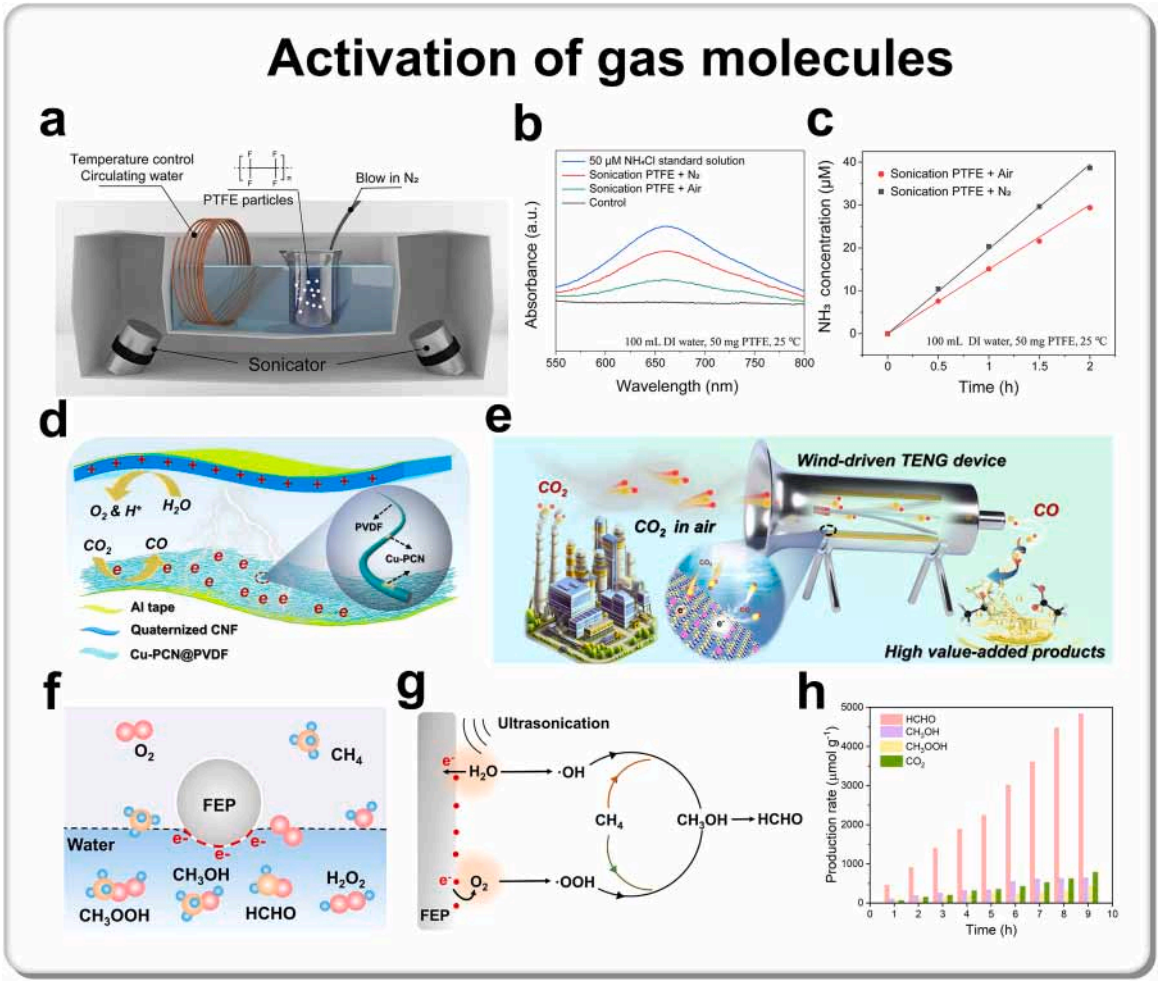

Fig. 8. Applications of CEC: Activation of gas molecules. (a) Schematic representation of the experimental setup. (b) Absorbance variations using the indophenol blue method under sonication with different atmospheres (100 mL DI water, 50 mg PTFE, 25 °C). (c) Comparison of NH_3 yields under air and N_2 at different ultrasonic times performed. Reproduced with permission [114]. Copyright 2024, Li et al. (d) Schematic diagram showing the structure of experimental setup. (e) Schematic illustration of CO_2 reduction process in air. Reproduced with permission [107]. Copyright 2024, Springer Nature. (f) Schematic of the experimental setup. (g) Proposed reaction mechanism for CH_4 conversion through CEC. (h) Results from the durability test of the PTFE over time. Reproduced with permission [53]. Copyright 2024, Wiley.

which the Faradaic efficiencies remained relatively constant, averaging 63.3% and 35.2%, respectively, providing a scalable device paradigm for distributed green carbon conversion, particularly toward multi-carbon products such as ethylene.

For methane (CH_4) activation, Li et al. [53] reported a new strategy for CH_4 oxidation under ambient conditions based on interfacial charge transfer (Fig. 8f), in which repeated CE between FEP and water under ultrasonic excitation enables efficient C-H bond activation at gas-liquid-solid three-phase interfaces (Fig. 8g), delivering formaldehyde (HCHO) and methanol (CH_3OH) yields of 467.5 and 151.2 μmol g^{-1}, respectively (Fig. 8h). Scale-up was further demonstrated using ten reactors connected in series, where stable product outputs were maintained (47.62 and 14.17 μmol of HCHO and CH_3OH, respectively), and after ten consecutive cycles, the methanol and formaldehyde yields remained at 93.2% and 94.4% of their initial values. Complementarily, Jia et al. [109] introduced polydopamine (PDA) into the system and employed oxygen-atmosphere photo-pretreatment to enrich strongly electron-withdrawing C═O functionalities on the PDA surface, achieving within 2 h formaldehyde and methanol yields of 1.5 mmol g^{-1} and 0.9 mmol g^{-1}, respectively, offering a scalable and mild route for C-H bond transformation.

Overall, above studies collectively delineate a clear evolutionary trajectory for gas molecule activation in CEC, spanning from nitrogen fixation toward nitrate, to multi-field-assisted and continuously sustained ammonia production, further extending to the capture and conversion of low-concentration CO_2 and the high-yield, scalable oxidation of CH_4 under mild conditions [53,107,112]. Looking ahead, key breakthroughs are expected to focus on enhancing selectivity and suppressing side reactions in complex gas-liquid-solid three-phase systems, achieving quantitative control and energy-efficiency assessment of interfacial charges and radical species, and deeply integrating CEC with continuous-flow reactors and downstream separation and purification units, advancing CE-driven gas activation toward scalable platforms for green chemical manufacturing and coupled carbon-nitrogen cycles.

3.5. Reduction of metal ions

Metal-ion reduction constitutes a pivotal step not only in precious-metal recovery and the synthesis of metal nanomaterials, but also as a key interfacial reaction pathway for converting "pollutants" into "resources" [52,116]. In CEC, mechanical stimulations such as ultrasonication induce interfacial electron transfer and accumulation at solid–liquid interfaces, driving metal-ion reduction and subsequent deposition or enrichment without an external power supply, or with a substantially reduced input of chemical reductants [117,118]. Meanwhile, the accessibility of reduction pathways is strongly governed by

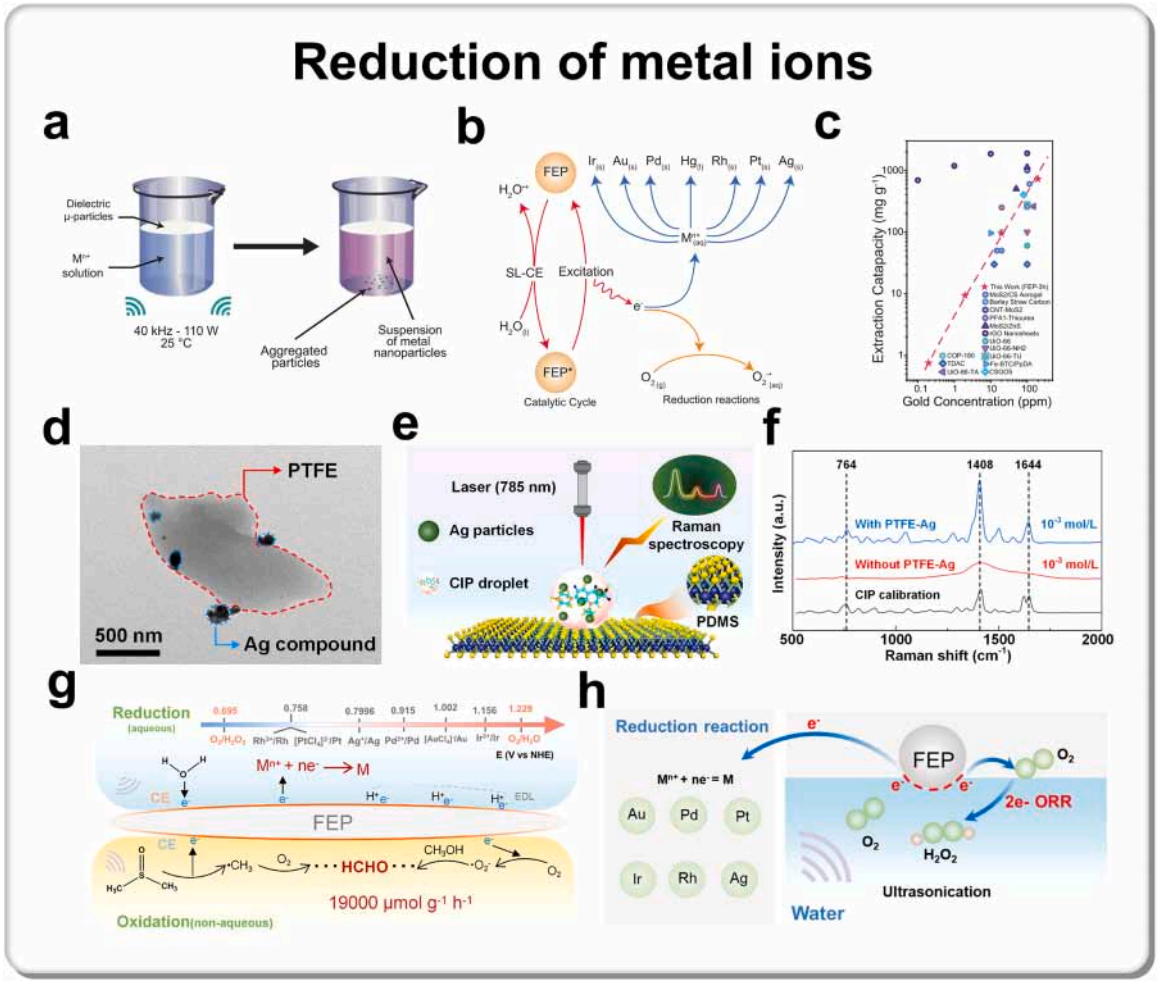

Fig. 9. Applications of CEC: Reduction of metal ions. (a) Graphical description of the experimental set-up for metal-ion extraction. (b) Schematic description of the reduction of various metal ions (M^{n+}) in aqueous solution by ultrasonically driven CEC in presence of FEP. (c) Au extraction capacity for FEP-based CEC compared to adsorption/reduction method using different materials, on a range from around 0.1 ppm to around 100 ppm. Reproduced with permission [52]. Copyright 2024, Springer Nature. (d) Transmission electron microscopy (TEM) image of PTFE and Ag composite. (e) The surface-enhanced Raman scattering (SERS) technology for ciprofloxacin (CIP) detection. (f) Corresponding SERS curve of the CIP. Reproduced with permission [117]. Copyright 2025, Elsevier. (g) Janus chemical processes in CEC. (h) Schematic of the reaction mechanism for metal ion reduction by CEC. Reproduced with permission [51]. Copyright 2025, American Chemical Society.

the intrinsic oxidative-reductive Janus character of the system, as well as by the surrounding atmosphere and the properties of the solvent and dielectric materials, collectively providing powerful design levers for achieving reaction selectivity [51].

Firstly, Su et al. [52] demonstrated that CEC enables metal-ion extraction over an exceptionally broad concentration window with high extraction capacity (Fig. 9a), wherein FEP microparticles in aqueous media directly generate the corresponding metal nanoparticles (for example, Au, Ag, Pt, Pd, Rh, and Ir; Fig. 9b). Specifically, Au extraction capacities spanning 0.756–722.5 mg g^{-1} was achieved within 3 h over an initial concentration range of 0.196–196 ppm (Fig. 9c), and atmosphere-controlled experiments further revealed that most metals exhibit higher reduction yields under anaerobic conditions, underscoring the robustness and generality of this approach for resource recovery. Building on this foundation, Li et al. [116] engineered TiO_2/PTFE composite microspheres and introduced an photonic field to enhance reaction, enabling gold recovery efficiencies of 97.6% and 96.3% from central processing unit (CPU) and random access memory (RAM) electronic wastes, respectively, marking a decisive transition from model solutions to complex solid-waste systems. Beyond recovery, metal-ion reduction via CEC also provides a versatile route for materials synthesis. For instance, Yan et al. [118] achieved rapid and size-tunable synthesis of Au nanoparticles at the water–PTFE interface under 150 W, 40 kHz ultrasound, with particle diameters controllably evolving from 74 to 220 nm by adjusting the reaction time from 1 to 20 min, revealing a well-defined kinetic synthesis window. In parallel, in situ metal reduction can be harnessed to construct functional interfaces: Zhou et al. [117] reduced Ag^+ directly on PTFE to form plasmonic Ag nanostructures (Fig. 9d), which enabled highly sensitive surface-enhanced Raman scattering (SERS) technology detection of ciprofloxacin (10^{-3} M) (Fig. 9e-f), exemplifying an integrated "reduction–material generation-application" paradigm.

From a mechanistic perspective, Wei et al. [51] elucidated the Janus oxidative-reductive nature of CEC (Fig. 9g) and quantitatively defined its reduction-accessible window between the $2e^-$ ORR ($E^0 = 0.695$ V vs NHE) and the $4e^-$ ORR ($E^0 = 1.229$ V vs NHE) (Fig. 9h), establishing a predictive reaction map and controllable variable space. Subsequently, Mohsin et al. [119] highlighted that metal-ion reduction efficiency is governed not only by the ability of dielectric materials to acquire electrons, but also by their propensity to donate electrons to ions or oxygen species in concert with solvent-dependent EDL screening. Notably, glass exhibits substantially higher charge transfer to Ag^+ than PTFE, and DMSO markedly amplifies reduction efficiency, offering an interpretable framework for synergistic design based on dielectric surface chemistry-solvent coupling. Finally, addressing more recalcitrant chelated metal systems, Shen and Chen et al. [120,121] independently employed CEC as a front-end decomplexation and transformation step for Cu(II)-EDTA and Co(II)-EDTA, followed by coupling with capacitive deionization or pH adjustment to complete metal recovery: the Cu system achieved 86.4% recovery within 150 min, whereas the Co system reached 41.6% decomplexation, exhibiting a kinetic constant of 0.024 min^{-1} and stable operation over 40 h, collectively demonstrating that CEC holds strong promise as a low-chemical-input pretreatment platform for the resource recovery of complexed metal-bearing wastewaters.

Overall, these studies collectively delineate a clear evolutionary trajectory for metal-ion reduction in CEC, progressing from the quantitative definition of reaction accessibility and control variables (such as atmosphere and potential thresholds), through high-capacity and broadly applicable extraction enabled by dielectric microparticles, to in situ nanomaterial synthesis [118], efficient recovery of precious metals from electronic waste [116], and the integrated decomplexation of chelated metal wastewaters [120,121]. Their shared value lies in harnessing mechanical energy to trigger interfacial electron transfer, thereby reducing reliance on external reductants or oxidants while maintaining quantifiable recovery efficiencies and robust process stability [52,119]. Looking forward, key breakthroughs are expected to focus on achieving selectivity in complex matrices (in the presence of coexisting ions and organic species), the directional utilization of the reductive–oxidative Janus character, and deep integration with continuous-flow and separation units, ultimately enabling scalable and deployable green platforms for metal resource recovery.

3.6. Recycling of spent lithium-ion batteries

Spent lithium-ion batteries represent not only a potential environmental liability but also an increasingly important "urban mine" rich in Li, Ni, Co, Mn and Fe [54,122,123]. Although conventional hydrometallurgical routes can deliver high leaching efficiencies and high-purity products, they typically rely on the continuous addition of external reducing agents (such as H_2O_2) and large dosages of chemical reagents, resulting in elevated operational costs, secondary effluent generation and safety concerns associated with reagent handling and storage [124–126]. By contrast, CEC-enabled recycling strategies harness mechanical energy to induce repetitive solid-liquid CE, enabling the generation of ROS, electrons or H_2O_2, thereby minimizing reliance on externally supplied reductants and offering a more sustainable and intrinsically safer pathway for green battery recycling [122,127].

Li et al. [122] were the first to embed a CEC process, exemplified by dielectric SiO_2 powders, into an organic-acid leaching framework, thereby demonstrating its broad applicability across multiple cathode chemistries (Fig. 10a). For lithium cobalt (III) oxide batteries, the leaching efficiency reached 100% for lithium and 92.19% for cobalt at 90 °C within 6 h. For ternary lithium batteries, the leaching efficiencies of lithium, nickel, manganese and cobalt reached 94.56%, 96.62%, 96.54% and 98.39% at 70 °C, respectively, within 6 h (Fig. 10b). Building on this foundation, subsequent materials engineering efforts rendered "interfacial charge-transfer capability" a tunable design parameter: fluorination of SiO_2 using FDTES produced F-SiO_2 (Fig. 10c), increasing the transferred charge from 4.67 nC to 28.58 nC and markedly enhancing ROS generation, which in turn elevated leaching efficiencies in ternary systems to 99.75% (Li), 99.44% (Ni), 96.77% (Co) and 94.07% (Mn), with stable performance over three reuse cycles (Fig. 10d) [54]. Moreover, Yang et al. [124] designed porous SiO_2 microspheres with a high specific surface area of 203.06 m^2 g^{-1}, approximately 117-fold greater than that of conventional SiO_2, thereby intensifying solid–liquid CE; combined with zwitterionic microstructures constructed via sodium alginate/polyethyleneimine (SA/PEI) modification, this approach promoted electron transfer and radical coupling, enabling near-quantitative leaching of Li, Co, Mn and Ni at 80 °C within 8 h, sustained over five cycles, alongside a cost assessment of US$ 19.27 kg^{-1} that underscored its economic viability. From a process-engineering perspective, Li et al. [125] further integrated high leaching efficiency with operational convenience by developing magnetically recoverable Fe_3O_4@SiO_2 materials, achieving Li/Co/-Ni/Mn leaching efficiencies of 98.3%/99.3%/98.3%/98.6% under 70 mg material loading, 0.4 M citric acid, 70 °C and 4 h, while maintaining negligible performance decay over five cycles, thus offering a more industry-compatible route for continuous operation. Finally, Zhang et al. [127] extended the CEC-enabled recycling paradigm beyond layered oxides to lithium iron phosphate (LFP) cathodes (Fig. 10e): using fluorinated polymers (FEP/PTFE/PTC) as recyclable materials to generate H_2O_2 in situ, they reduced the reaction enthalpy from 407 to 288 kJ mol^{-1} and boosted the H_2O_2 generation rate to 164 mmol L^{-1} g^{-1} h^{-1} (Fig. 10f), thereby enabling rapid recovery of Li (99.8%) and Fe (99.97%) within 8 min at 50 °C and highlighting the high efficiency and promising economic prospects of CEC-based LFP recycling.

Collectively, these studies delineate a coherent technological evolution of CEC-driven lithium-ion battery recycling: beginning with dielectric SiO_2 powders that enable in situ reduction/activation, progressing to surface fluorination strategies that enhance interfacial

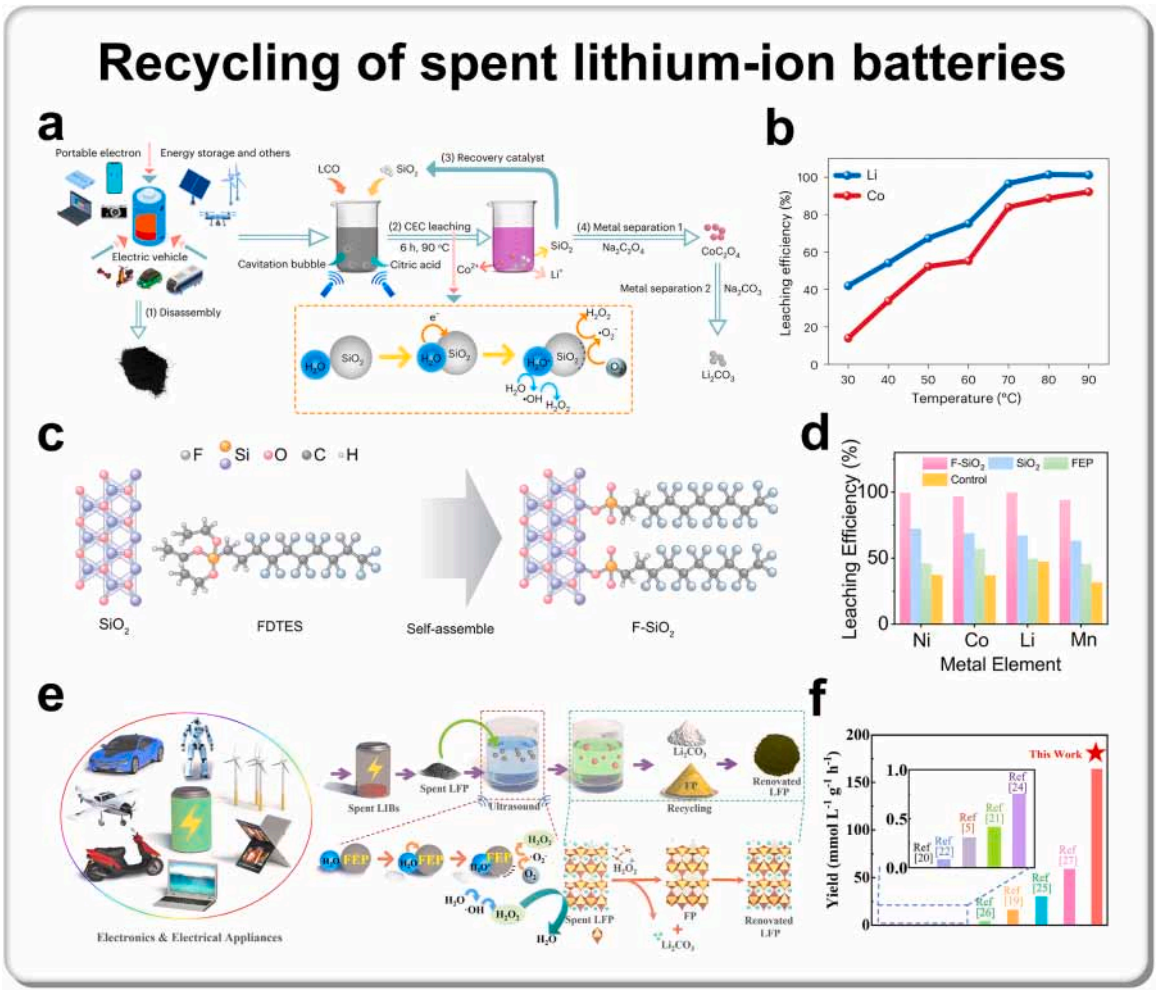

Fig. 10. Applications of CEC: Recycling of spent lithium-ion batteries. (a) Flow chart of lithium battery recovery by CEC leaching. (b) Leaching efficiencies of Li and Co at different temperatures. Reproduced with permission [122]. Copyright 2023, Springer Nature. (c) Schematic illustration of the fluorination process on the SiO_2 surface. FDTES refers to 1 H,1 H,2 H,2H-perfluorodecyltriethoxysilane. (d) Corresponding leaching efficiencies of different metal elements in each group. Reproduced with permission [54]. Copyright 2025, Springer Nature. (e) The overall recycling process of spent lithium iron phosphate (LFP) batteries via CEC. (f) The comparative analysis of H_2O_2 yield. Reproduced with permission [127]. Copyright 2025, Wiley.

charge transfer, followed by the synergistic coupling of microstructural design and surface chemical environments to amplify ROS and electron generation, and further advancing toward magnetically recoverable or regenerable materials that lower separation and recycling costs, ultimately extending applicability to mainstream cathode systems such as LFP. The shared merit of these approaches lies in harnessing mechanical energy to trigger interfacial reactions, thereby reducing the reliance on externally added reductants and excessive chemical inputs while maintaining high leaching efficiencies and material reusability, collectively providing a validated materials and process foundation for lower-carbon, safer and more readily closed-loop recycling of spent lithium-ion batteries.

3.7. Other applications

Beyond pollutant degradation, H_2O_2 production, gas molecule activation, and metal resource recovery, CEC has also been extensively explored in materials synthesis [8,58,128], seawater uranium extraction [129,130], chemiluminescence and chemical analysis [131–134], as well as hydrogen evolution [94,135,136]. Although these studies span disparate targets, from polymers and nuclear resources to analytical chemistry and hydrogen energy, they share a common physical-chemical foundation: mechanical perturbation at dielectric-liquid interfaces induces interfacial charge transfer and accumulation, which subsequently triggers the generation of ROS and the establishment of intense interfacial electric fields [57,137–139]. These coupled processes enable controllable chemical reactions to proceed under mild conditions, with reaction intensity and efficiency further tunable and amplifiable through deliberate engineering of surface chemistry, material structure, and external mechanical fields [55, 140].

From the perspective of polymer synthesis, Li et al. [8] demonstrated that the oxidative polymerization of aniline can be driven by FEP dielectric materials under mild conditions (Fig. 11a), eliminating the need for strong oxidants or externally applied electric fields and providing a sustainable alternative for the preparation of conducting polymers. Extending this strategy, Wang et al. [58] achieved well-controlled polymerization under gentle mechanical agitation by maintaining a stable Cu(II)/Cu(I) redox equilibrium. At a stirring frequency of 7 Hz, the reaction reached ~80% monomer conversion within 24 h and produced polymers with a narrow dispersity ($Đ = 1.16$) and a relatively high molecular weight ($M_n = 12900$). These results highlight the progression of CEC from a simple polymerization trigger toward a powerful tool for regulating polymerization kinetics and tailoring product distributions. In addition, Chen et al. [128] employed black phosphorus quantum dots (BP QDs) as precursors to fabricate a nanomedicine with highly exposed phosphate groups (EM-eNMs) via CEC, which can serve as an analogue of inorganic polyphosphates that play

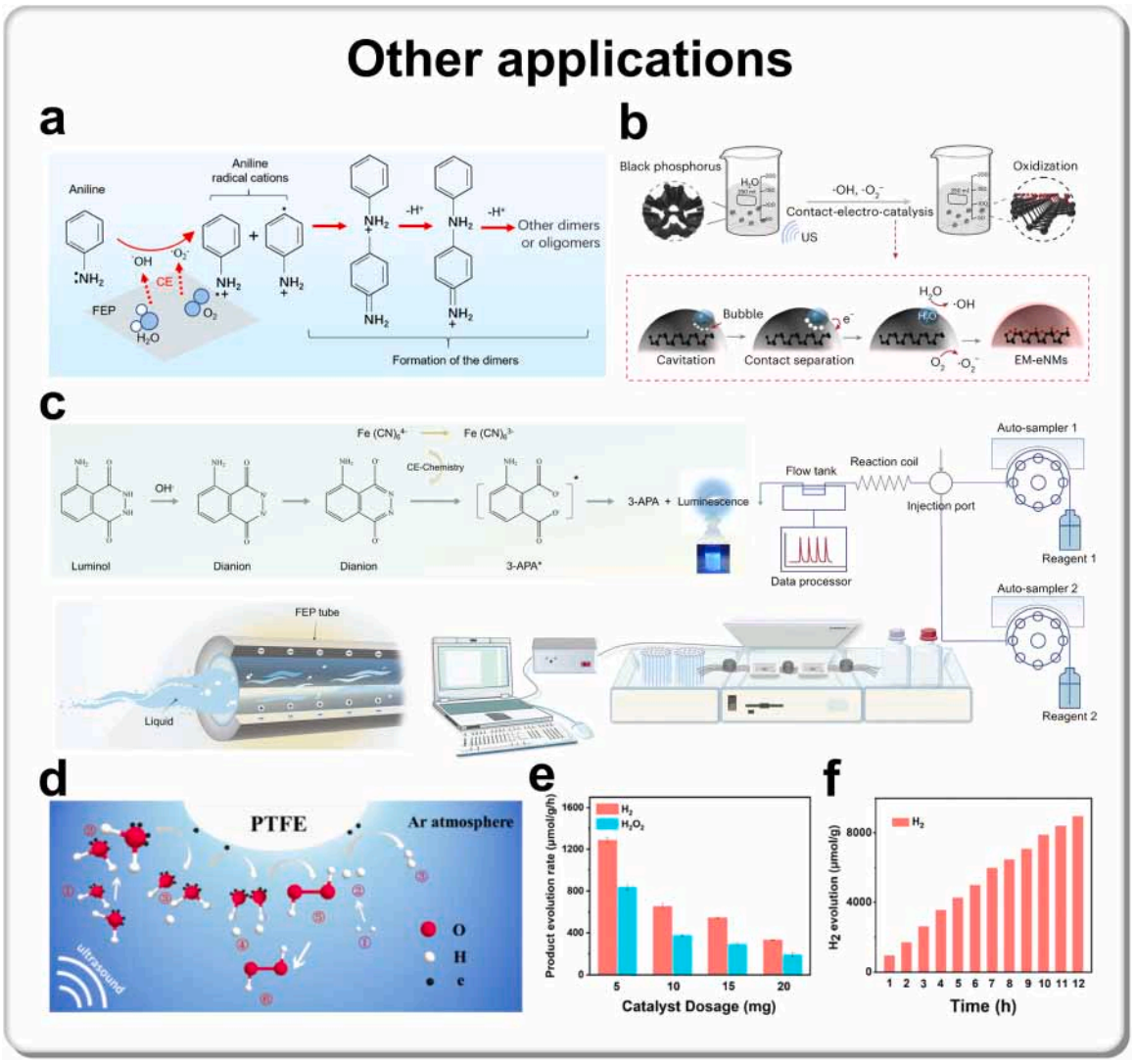

Fig. 11. Significant application of CEC: other applications. (a) Schematic of aniline polymerization induced by CEC. Reproduced with permission [8]. Copyright 2024, Elsevier. (b) Schematic illustration of CEC preparation of energy metabolism-engaged nanomedicines (EM-eNMs). Reproduced with permission [128]. Copyright 2025, Springer Nature. (c) Overview of flow injection analysis (FIA) sample detection system for luminol luminescence during CEC. Reproduced with permission [133]. Copyright 2025, Springer Nature. (d) Schematic diagram of CEC water oxidation and proton reduction. (e) Comparison of the average production rates of H_2 and H_2O_2 within 2 h for different amounts of PTFE. (f) Durability experiment, in which the H_2 production over PTFE was tested for 12 consecutive hours. Reproduced with permission [136]. Copyright 2025, The Royal Society of Chemistry.

key roles in energy-metabolism-related processes. Unlike conventional oxidative routes that directly degrade BP quantum dots into phosphates, this process enables a controlled evolution of surface-oxidized structures, effectively promoting the formation of EM-ENMs. Mechanistically, the hydrophilic surface of the EM-eNMs facilitates hydration reactions, which suppress repeated contact and separation between the nanomaterials and water, while the highly exposed surface phosphate groups act as protective and terminating layers, preventing radical-induced oxidative degradation and preserving the structural integrity of the EM-eNMs (Fig. 11b). Collectively, this class of studies demonstrates that CEC is not limited to small-molecule transformations, but also provides a versatile energy input and pathway to control strategy for polymer synthesis and nanomaterials engineering.

In the field of uranium extraction from aqueous solutions and seawater, a clear progression can be observed, ranging from model solutions to real seawater systems, and from extraction efficiency to antifouling performance [129,130]. In aqueous systems, Liu et al. [129] demonstrated that PTFE can generate electrons and ROS under ultrasonic conditions, converting U(VI) into precipitable products and achieving high removal efficiencies, while maintaining effective extraction in real uranium-containing wastewater. Extending this approach to seawater, Dai et al. [130] exploited the low-adhesion and self-cleaning properties of hydrophobic PTFE to facilitate the timely detachment of uranium products, while the concomitantly generated ROS impart antifouling capability, enabling high extraction efficiency, enhanced selectivity, and good cycling stability under complex marine conditions and long-term operation. Overall, these studies demonstrate that CEC can serve as a low-chemical-input driving force for seawater resource recovery, with surface engineering effectively addressing key engineering bottlenecks such as product passivation and biofouling.

The essence of luminol chemiluminescence/electrochemiluminescence lies in the efficient and controllable generation of ROS or oxidative intermediates [131,132]. However, conventional approaches often rely on externally added H_2O_2, metal/enzymatic catalysts, or are constrained by electrochemical windows and parasitic side reactions [133,134]. Recent studies demonstrate that interfacial charge transfer induced by CE can trigger ROS generation at interfaces, transforming the luminescence process into a tunable and amplifiable

analytical signal. For example, Xu et al. [131] employed ROS generated at an ultrasonically driven FEP–water interface to directly activate luminol. Unlike conventional luminol chemiluminescence dominated by a single emission peak at 425 nm, the contact-electrification-induced luminescence (CEL) system enables direct observation of two emission bands at 425 and 475 nm, corresponding to distinct reaction intermediates and thus realizing intermediate visualization, providing a new paradigm for mechanistic elucidation of luminol luminescence and for constructing tunable luminescent signals in environmental and bioanalytical applications. In addition, at the level of signal amplification and sensing, Zhong et al. [132] further developed a turn-off/on platform, enabling sensitive detection of superoxide dismutase (SOD) (0.0050–2.0 μg mL^{-1}) and thiabendazole (TBZ) (0.500–60.0 μM) with good reproducibility and applicability to real samples. Meanwhile, targeting continuous and online chemical analysis, Xu et al. [133] extended CEC to flow electrification in dielectric tubing, engineering reaction rates by tuning tube diameter, length, flow rate, and series/parallel configurations, and mimicking flow injection analysis (FIA) to design cascaded reactions: pump I oxidizes $[Fe(CN)_6]^{4-}$ within an FEP tube to generate catalytically active species, while pump II simultaneously drives luminol oxidation and emission, with maximal fluorescence observed upon mixing the two streams (Fig. 11c), demonstrating a flow-based implementation of "programmable cascade reactions".

CEC can also be extended to hydrogen production [135,136]. For example, Tian et al. [136] demonstrated a pure-water hydrogen generation strategy, showing that PTFE alone can sustain hydrogen evolution under mechanical excitation with a rate of 1286.6 mmol g^{-1} h^{-1} (Fig. 11d), accompanied by the concurrent formation of H_2O_2 at 837.9 mmol g^{-1} h^{-1} (Fig. 11e) and a cumulative hydrogen yield of 8952.7 mmol g^{-1} over 12 h (Fig. 11f), highlighting the potential of an extremely simplified material system and reaction configuration with sustained activity. Complementarily, Wang et al. [135] developed transition-metal-doped Bi_5O_7I as a hydrogen evolution material, demonstrating that dopant-induced modulation of water adsorption and electronic structure can markedly enhance vibration-driven hydrogen evolution, underscoring the importance of material designability within CEC systems. Together, these studies indicate that future breakthroughs in hydrogen production will rely not only on the quantitative control of interfacial charge and ROS fluxes, but also on the engineering optimization of material electronic structures and interfacial active sites.

Based above works, a clearer picture emerges in which CEC is evolving from its initial focus on environmental remediation and resource recovery toward broader applications in synthetic manufacturing, analytical detection, and hydrogen energy conversion, progressively adopting a more designable, scalable, and integrable technological form [8,128,130,133,136]. Looking ahead, key cross-cutting advances are expected to center on the quantitative characterization of interfacial charge transfer and ROS generation, the control of selectivity and suppression of side reactions in complex media, and the deep integration of CEC with continuous-flow reactors and downstream separation or online analytical units, ultimately advancing contact-electrification-driven interfacial chemistry into a universally deployable platform technology.

4. Conclusion and prospect

In this review, we summarize the conceptual basis, fundamental principles, key characteristics, and representative applications of CEC, and describe how this field has progressed from a largely overlooked interfacial physical phenomenon to a reaction framework that can be systematically analyzed and engineered. Mechanistic models reported to date, including the widely adopted "two-step" reaction model in aqueous and organic systems, are examined from three closely linked perspectives: interfacial charge transfer and accumulation, interfacial electric fields, and ROS generation. Representative advances of CEC in organic pollutant degradation (organic dye degradation, phenolic pollutant degradation, antibiotics degradation, etc.), biomedical applications, direct synthesis of H_2O_2, activation of gas molecules, reduction of metal ions, recycling of spent lithium-ion batteries, materials synthesis, seawater uranium extraction, chemiluminescence, as well as hydrogen evolution are systematically reviewed. According to surveyed CEC studies, 71% of reported reactions involve oxidation, whereas only 29% involve reduction, indicating that the predominance of oxidation processes arises from the intrinsic asymmetry of interfacial charge transfer. In most systems, CEC is initiated by electron donation from liquid molecules to solid surfaces, constituting an oxidation step. The accumulated interfacial electrons are then preferentially consumed by dissolved oxygen to generate reactive oxygen species rather than transferred to reducible substrates, making oxidative pathways dominant. In contrast, reduction reactions require more stringent conditions, including prolonged electron lifetime, suppressed oxygen competition, favorable substrate adsorption, and directed electron-transfer pathways, which remain insufficiently developed in current CEC systems. It is also important to distinguish CEC from related mechano-driven or interfacial reaction concepts. Although ultrasound is frequently used to trigger CEC, classical sonochemistry is primarily governed by acoustic cavitation and hot-spot chemistry, whereas CEC is defined by CE-induced charge transfer and the resulting localized electric field at interfaces. Likewise, although CEC shares with microdroplet chemistry the broader features of interfacial reactivity and strong electric fields, microdroplet chemistry is generally discussed in terms of gas-liquid or liquid-liquid interfacial acceleration involving asymmetric solvation, concentration enrichment, curvature, evaporation, and nonequilibrium charge distributions. Recent studies nevertheless suggest that CE may contribute to intrinsic electrification of microdroplets under certain conditions [141,142]. These observations indicate that sonochemistry, microdroplet chemistry, and CEC are best viewed as complementary but distinct in mechanism within the broader landscape of interfacial chemistry. Moreover, compared with electrocatalysis and photocatalysis, CEC should be regarded as a mechanistically independent yet complementary catalytic platform. Whereas electrocatalysis and photocatalysis rely on externally applied bias or photon input to generate reactive charge carriers, CEC is driven by mechanically induced, transient interfacial charge transfer during contact-separation processes. In this sense, CEC does not replace photocatalysis or electrocatalysis, but rather expands the catalytic landscape by introducing an alternative route for chemical activation based on interfacial electrification. Existing studies have shown that this mechanism enables CEC to operate without electrodes or highly specific catalytic materials. These characteristics endow CEC with distinct advantages over conventional technologies, including mild reaction conditions, broad material compatibility, and spatiotemporal decoupling of redox reactions, marking its transition from conceptual proof-of-principle to a designable reaction platform centered on interfacial regulation. In addition, current results suggest that CEC has already demonstrated practical potential in certain systems, combining high reaction efficiency, useful selectivity, recyclable materials, and encouraging process economics. Nevertheless, its broader implementation still faces many challenges, as discussed below:

First, at the level of materials design, current studies still rely predominantly on macroscopic triboelectric materials, and future efforts should move toward more refined control of interfacial electronic structures. This includes the incorporation of metal nanoclusters, single-atom sites, framework materials (such as MOFs, COFs, and HOFs), and two-dimensional materials (e.g., MXene, and graphene), as well as their composites, to establish well-defined electron-donating/accepting sites and tunable interfacial properties (including confinement effects, ion selectivity, and surface wettability). Such strategies will enable more precise regulation of the directionality of interfacial electron transfer and ion migration, reaction selectivity, and the identity of generated ROS.

Second, in terms of characterization techniques, there is a pressing need for in situ methods capable of directly probing the strength and

spatial distribution of interfacial electric fields, charge-transfer dynamics, and the formation and evolution of reaction intermediates. When combined with ex situ chemical analyses, these approaches will allow spatially and temporally resolved identification of where reactions occur and how they proceed, reducing the reliance on post-reaction product analysis alone to infer interfacial mechanisms.

With respect to interfacial microenvironment regulation, the efficiency and sustainability of CEC are highly sensitive to local conditions. Beyond conventional variables such as atmosphere and pH, organic aprotic solvent systems offer distinct advantages in suppressing ionic screening and prolonging charge transfer lifetimes. In particular, under high ionic strength conditions, the EDL can rapidly screen surface charges and thereby significantly impede subsequent electron-transfer processes. And the roles of cation-anion effects and their dynamic evolution remain to be systematically clarified.

At present, many CEC studies still rely on practically accessible proxy reactions and indirect descriptors for performance comparison. For example, methyl orange degradation has been widely adopted as a standard probe reaction for benchmarking CEC kinetics, while radical generation is commonly characterized by radical scavengers, trapping methods, or fluorescence probes. These approaches provide a useful and currently feasible basis for comparing different systems. However, important descriptors and evaluation metrics, such as local charge density, electric field strength, criteria for distinguishing oxidative versus reductive reaction pathways, the development of an "equivalent Faradaic efficiency" concept suitable for electrode-free systems, and reaction flux normalized to the effective active interfacial area, chemical output normalized to mechanical energy input, remain difficult to define and directly quantify at present. This challenge arises in part from the electrode-free nature of CEC, which makes in situ characterization less straightforward than in electrocatalysis or photocatalysis. Thus, the current evaluation framework should be regarded as a necessary transitional stage. With the future advancement of characterization techniques and testing methodologies, we anticipate that these important descriptors and performance metrics for CEC will be progressively defined and more widely incorporated into the field.

In addition, substantial opportunities remain in system diversification and synergistic catalysis. Beyond commonly employed ultrasonication, liquid flow, ball milling, stir, and macroscopic droplet motion, contact-separation processes at three-phase interfaces involving microdroplets and microbubbles are expected to serve as highly efficient induction modes for CEC. These configurations can be further coupled synergistically with light, thermal, piezoelectric, or ferroelectric effects to expand the reaction window and improve overall energy efficiency. Moreover, through reaction modularization, array-based integration, and continuous-flow scale-up, the conversion of transient interfacial events into stable and controllable chemical fluxes will be a critical step toward translating CEC from a laboratory phenomenon into a viable engineering technology.

Taken together, with coordinated advances in materials, characterization, interfacial regulation, and system-level design, CEC is well positioned to evolve into a general interfacial reaction platform with both theoretical predictability and practical scalability.

CRediT authorship contribution statement

Han Qian: Writing – original draft, Investigation, Formal analysis, Conceptualization. **Zhong Lin Wang:** Writing – review & editing, Conceptualization. **Di Wei:** Writing – review & editing, Funding acquisition, Formal analysis, Conceptualization.

Declaration of Competing Interest

The authors declare that they have no known competing financial interests or personal relationships that could have appeared to influence the work reported in this paper.

Acknowledgements

This work was supported by the National Natural Science Foundation (Grant No. 22479016).

Data availability

No data was used for the research described in the article.

References

[1] S. Lin, X. Chen, Z.L. Wang, Contact electrification at the liquid–solid interface, Chem. Rev. 122 (2022) 5209–5232, https://doi.org/10.1021/acs.chemrev.1c00176.
[2] S. Lin, L. Xu, A. Chi Wang, Z.L. Wang, Quantifying electron-transfer in liquid-solid contact electrification and the formation of electric double-layer, Nat. Commun. 11 (2020) 399, https://doi.org/10.1038/s41467-019-14278-9.
[3] Y. Du, Z.L. Wang, D. Chu, G. Amaratunga, D. Wei, Iontronics for adaptive and flexible pressure sensing, Iontronics 2 (2026) 13, https://doi.org/10.20517/iontronics.2026.13.
[4] L.S. McCarty, G.M. Whitesides, Electrostatic charging due to separation of ions at interfaces: contact electrification of ionic electrets, Angew. Chem. Int. Ed. 47 (2008) 2188–2207, https://doi.org/10.1002/anie.200701812.
[5] Y. Zhao, Y. Liu, Y. Wang, S. Li, Y. Liu, Z.L. Wang, P. Jiang, The process of free radical generation in contact electrification at solid-liquid interface, Nano Energy 112 (2023) 108464, https://doi.org/10.1016/j.nanoen.2023.108464.
[6] S. Li, J. Liu, Z.L. Wang, D. Wei, Mechano-driven chemical reactions, Green. Energy Environ. 10 (2025) 937–966, https://doi.org/10.1016/j.gee.2024.08.001.
[7] S.T. Muntaha, Z.L. Wang, D. Wei, Reevaluating mechano-driven chemical reactions: insights from ultrasonic, piezo, and contact-electro mechanisms, Electrochim. Acta 544 (2025) 147563, https://doi.org/10.1016/j.electacta.2025.147563.
[8] S. Li, Z. Zhang, P. Peng, X. Li, Z.L. Wang, D. Wei, A green approach to induce and steer chemical reactions using inert solid dielectrics, Nano Energy 122 (2024) 109286, https://doi.org/10.1016/j.nanoen.2024.109286.
[9] Y. Wu, Y. Liu, C. Zhu, X.-Y. Kong, L. Wen, Olfactory-inspired nanofluidic sensor: molecular recognition and transport in confined space, Iontronics 2 (2026) 14, https://doi.org/10.20517/iontronics.2026.001.
[10] M. Liu, X. Wu, P.J. Dyson, Tandem catalysis enables chlorine-containing waste as chlorination reagents, Nat. Chem. 16 (2024) 700–708, https://doi.org/10.1038/s41557-024-01462-8.
[11] I.A. Moreno-Hernandez, B.S. Brunschwig, N.S. Lewis, Crystalline nickel, cobalt, and manganese antimonates as electrocatalysts for the chlorine evolution reaction, Energy Environ. Sci. 12 (2019) 1241–1248, https://doi.org/10.1039/C8EE03676D.
[12] J. Yang, W.-H. Li, H.-T. Tang, Y.-M. Pan, D. Wang, Y. Li, CO2-mediated organocatalytic chlorine evolution under industrial conditions, Nature 617 (2023) 519–523, https://doi.org/10.1038/s41586-023-05886-z.
[13] K. Zuraiqi, A. Zavabeti, J. Clarke-Hannaford, B.J. Murdoch, K. Shah, M.J. S. Spencer, C.F. McConville, T. Daeneke, K. Chiang, Direct conversion of CO2 to solid carbon by Ga-based liquid metals, Energy Environ. Sci. 15 (2022) 595–600, https://doi.org/10.1039/D1EE03283F.
[14] H. Ling, X.-Y. Kong, L. Wen, Ionic superfluidics: a perspective on emerging frameworks for ion transport in confined channels, Iontronics 1 (2025) 6, https://doi.org/10.20517/iontronics.2025.06.
[15] X. Zhu, Z. Wu, Z. Zhao, Bio-inspired heterointerfacial ion-gating and iontronic neuromorphics, Iontronics 1 (2025) 4, https://doi.org/10.20517/iontronics.2025.04.
[16] Z. Wang, X. Dong, W. Tang, Z.L. Wang, Contact-electro-catalysis (CEC), Chem. Soc. Rev. 53 (2024) 4349–4373, https://doi.org/10.1039/D3CS00736G.
[17] J. Li, J. Yin, W. Guo, Hydrovoltaic energy and intelligence: where ions meet electrons, Iontronics 1 (2025) 3, https://doi.org/10.20517/iontronics.2025.03.
[18] X. Li, Z.L. Wang, D. Wei, Iontronic logic control driven by dynamic electrical double layer regulation, Iontronics 1 (2025) 2, https://doi.org/10.20517/iontronics.2025.02.
[19] A. Wang, S. Feng, T. Xiao, G. Wang, B. Zhu, W. Zhou, L. Wang, Microenvironment-engineered piezoionic hydrogel nanogenerators for enhanced energy harvesting and sensing, SmartSys 1 (2025) e70004, https://doi.org/10.1002/sys3.70004.
[20] X. Chen, Y. Liu, T. Deng, M. Wang, Bioinspired mechanosensitive ion channels: design principles and emerging applications, Iontronics 2 (2026) 12, https://doi.org/10.20517/iontronics.2026.12.
[21] C. Chen, H. Jin, P. Wang, X. Sun, M. Jaroniec, Y. Zheng, S.-Z. Qiao, Local reaction environment in electrocatalysis, Chem. Soc. Rev. 53 (2024) 2022–2055, https://doi.org/10.1039/D3CS00669G.
[22] Y. Su, A. Berbille, Z.L. Wang, W. Tang, Water-solid contact electrification and catalysis adjusted by surface functional groups, Nano Res 17 (2024) 3344–3351, https://doi.org/10.1007/s12274-023-6125-9.
[23] Z. Shen, D. Zhu, M. Zhang, Synergy of smart materials and structures toward intelligent metamaterials, SmartSys 1 (2025) e70007, https://doi.org/10.1002/sys3.70007.

[24] Z. Sun, T. He, Z. Ren, C. Wang, X. Liu, Z. Zhang, J. Zhou, X. Guo, Y. Yang, C. Lee, Moving toward human-like perception and sensation systems—from integrated intelligent systems to decentralized smart devices, SmartSys 1 (2025) e4, https://doi.org/10.1002/sys3.4.

[25] R. Zhang, Triboelectric intelligence, SmartSys 1 (2025) e2, https://doi.org/10.1002/sys3.2.

[26] B. Zhou, Q. Zhou, Z. Liu, X. Zhou, L. Bao, Engineering artificial spider silk from biomimetic synthesis to advanced applications, SmartSys 1 (2025) e70005, https://doi.org/10.1002/sys3.70005.

[27] J.C. Sobarzo, F. Pertl, D.M. Balazs, T. Costanzo, M. Sauer, A. Foelske, M. Ostermann, C.M. Pichler, Y. Wang, Y. Nagata, M. Bonn, S. Waitukaitis, Spontaneous ordering of identical materials into a triboelectric series, Nature 638 (2025) 664–669, https://doi.org/10.1038/s41586-024-08530-6.

[28] M.W. Williams, Triboelectric charging of insulators—evidence for electrons versus ions, IEEE Trans. Ind. Appl. 47 (2011) 1093–1099, https://doi.org/10.1109/TIA.2011.2126032.

[29] T.A.L. Burgo, T.R.D. Ducati, K.R. Francisco, K.J. Clinckspoor, F. Galembeck, S. E. Galembeck, Triboelectricity: macroscopic charge patterns formed by self-arraying ions on polymer surfaces, Langmuir 28 (2012) 7407–7416, https://doi.org/10.1021/la301228j.

[30] S. Li, J. Nie, Y. Shi, X. Tao, F. Wang, J. Tian, S. Lin, X. Chen, Z.L. Wang, Contributions of different functional groups to contact electrification of polymers, Adv. Mater. 32 (2020) 2001307, https://doi.org/10.1002/adma.202001307.

[31] Z. Wang, A. Berbille, Y. Feng, S. Li, L. Zhu, W. Tang, Z.L. Wang, Contact-electro-catalysis for the degradation of organic pollutants using pristine dielectric powders, Nat. Commun. 13 (2022) 130, https://doi.org/10.1038/s41467-021-27789-1.

[32] J. Liu, Z. Yang, S. Li, Y. Du, Z. Zhang, J. Shao, M. Willatzen, Z.L. Wang, D. Wei, Nonaqueous contact-electro-chemistry via triboelectric charge, J. Am. Chem. Soc. 146 (2024) 31574–31584, https://doi.org/10.1021/jacs.4c09318.

[33] J. Liu, Z. Yang, S. Li, H. Qian, T. Gan, N. Wu, Z.L. Wang, D. Wei, Modular contact-electro-chemistry based on dielectrics with work function-tunable metal coatings, Nano Energy 144 (2025) 111389, https://doi.org/10.1016/j.nanoen.2025.111389.

[34] X. Dong, Z. Wang, Y. Hou, Y. Feng, A. Berbille, H. Li, Z.L. Wang, W. Tang, Regulating contact-electro-catalysis using polymer/metal janus composite catalysts, J. Am. Chem. Soc. 146 (2024) 28110–28118, https://doi.org/10.1021/jacs.4c07446.

[35] R. Wang, W. Li, S. Wang, B. Du, X. Bai, H. Yan, D. Gao, X. Ren, W. Guo, F.R. Fan, G.Z. Chen, Directional electron transfer in island-sea structured contact-electro-catalysis enables cascade defluorination of PFAS, Angew. Chem. Int. Ed. 65 (2026) e25861, https://doi.org/10.1002/anie.202525861.

[36] Y. Wang, J. Zhang, W. Zhang, J. Yao, J. Liu, H. He, C. Gu, G. Gao, X. Jin, Electrostatic field in contact-electro-catalysis driven C−F bond cleavage of perfluoroalkyl substances, Angew. Chem. Int. Ed. 63 (2024) e202402440, https://doi.org/10.1002/anie.202402440.

[37] J.-M. McGregor, J.T. Bender, A.S. Petersen, L. Cañada, J. Rossmeisl, J. F. Brennecke, J. Resasco, Organic electrolyte cations promote non-aqueous CO2 reduction by mediating interfacial electric fields, Nat. Catal. 8 (2025) 79–91, https://doi.org/10.1038/s41929-024-01278-2.

[38] Z. Wang, I. Kulikov, T. Mustafa, S. Schott, R.L. Carey, J. Behrends, H. Sirringhaus, Electrically detected magnetic resonance in ambipolar polymer field-effect transistors, Phys. Rev. Lett. 135 (2025) 166301, https://doi.org/10.1103/7b3m-8zvz.

[39] D.M. Ma, W. Li, J. Zhang, K.C. He, C.Y. Zhang, G. Wang, X.D. Xin, Q. Liu, F. L. Cheng, S.H. Lv, D.F. Xing, Fluorocarbon polymers mediated contact-electro-catalysis activating peroxymonosulfate for emerging pollutants degradation: the key role of fluorine density in electron transfer, Chem. Eng. J. 497 (2024), https://doi.org/10.1016/j.cej.2024.154996.

[40] K. Grace Pavithra, P. Sundar Rajan, J. Arun, K. Brindhadevi, Q. Hoang Le, A. Pugazhendhi, A review on recent advancements in extraction, removal and recovery of phenols from phenolic wastewater: challenges and future outlook, Environ. Res. 237 (2023) 117005, https://doi.org/10.1016/j.envres.2023.117005.

[41] Y. Lai, K. Li, S. Lin, L. Zhou, Z. Yu, Y. Yuan, Contact-electro-catalysis triggers peroxymonosulfate activation for micropollutant degradation, Sci. China Technol. Sci. 68 (2025) 1720502, https://doi.org/10.1007/s11431-025-2950-1.

[42] P. Yadav, S. Manori, R.K. Shukla, Contact electro catalysis driven degradation of malachite green dye by RGO/ZnO nanohybrid, Solid State Commun. 389 (2024) 115578, https://doi.org/10.1016/j.ssc.2024.115578.

[43] W.-Z. Song, M. Zhang, H.-J. Qiu, C.-L. Li, T. Chen, L.-L. Jiang, M. Yu, S. Ramakrishna, Z.-L. Wang, Y.-Z. Long, Insulator polymers achieve efficient catalysis under visible light due to contact electrification, Water Res 226 (2022) 119242, https://doi.org/10.1016/j.watres.2022.119242.

[44] T. Gan, Z. Li, S. Li, H. Liu, G. Amaratunga, Z. Wang, D. Wei, Sustainable fluorinated silicon dielectric design for enhanced contact-electro-chemistry, Angew. Chem. Int. Ed. 64 (2025) e202517059, https://doi.org/10.1002/anie.202517059.

[45] X. Dong, Z. Wang, A. Berbille, X. Zhao, W. Tang, Z.L. Wang, Investigations on the contact-electro-catalysis under various ultrasonic conditions and using different electrification particles, Nano Energy 99 (2022) 107346, https://doi.org/10.1016/j.nanoen.2022.107346.

[46] X. Li, W. Tong, J. Shi, X. Zhang, Y. Chen, X. Liu, Y. Zhang, Contact-electro-catalysis through electret behavior to facilitate electron transfer, ACS Appl. Mater. Interfaces 16 (2024) 42293–42304, https://doi.org/10.1021/acsami.4c09206.

[47] Z. Wu, S. Wu, L. Zhang, Z. Wu, S. Hong, B. Chen, G. Zhu, Y. Jia, Low-frequency contact-electro-catalysis driven by friction between the PTFE-coated fabric and dye solution, J. Alloy. Compd. 1010 (2025) 177440, https://doi.org/10.1016/j.jallcom.2024.177440.

[48] C. Shu, M. He, Z. Wang, Z.L. Wang, Organic pollutants degradation based on poled dielectric films by contact-electro-catalysis, J. Phys. Chem. C. 129 (2025) 9699–9705, https://doi.org/10.1021/acs.jpcc.5c00485.

[49] Z. Wang, X. Dong, X.-F. Li, Y. Feng, S. Li, W. Tang, Z.L. Wang, A contact-electro-catalysis process for producing reactive oxygen species by ball milling of triboelectric materials, Nat. Commun. 15 (2024) 757, https://doi.org/10.1038/s41467-024-45041-4.

[50] Z. Liu, Z. Wang, K. Shi, H. Li, Y. Su, W. Han, Z.L. Wang, W. Tang, Contact-electro-catalysis at dynamic semiconductor–water junctions, Research 8 (2025) 0940, https://doi.org/10.34133/research.0940.

[51] T. Gan, Z. Yang, S. Li, H. Qian, Z. Li, J. Liu, P. Peng, J. Bai, H. Liu, Z. Wang, D. Wei, Unveiling Janus chemical processes in contact-electro-chemistry through oxygen reduction reactions, J. Am. Chem. Soc. 147 (2025) 25407–25416, https://doi.org/10.1021/jacs.5c05124.

[52] Y. Su, A. Berbille, X.-F. Li, J. Zhang, M. PourhosseiniAsl, H. Li, Z. Liu, S. Li, J. Liu, L. Zhu, Z.L. Wang, Reduction of precious metal ions in aqueous solutions by contact-electro-catalysis, Nat. Commun. 15 (2024) 4196, https://doi.org/10.1038/s41467-024-48407-w.

[53] W. Li, J. Sun, M. Wang, J. Xu, Y. Wang, L. Yang, R. Yan, H. He, S. Wang, W.-Q. Deng, Z.-Q. Tian, F.R. Fan, Contact-electro-catalysis for direct oxidation of methane under ambient conditions, Angew. Chem. Int. Ed. 63 (2024) e202403114, https://doi.org/10.1002/anie.202403114.

[54] Z. Wang, X. Dong, N. Wu, Y. Feng, X. Yang, H. Li, Z. Yang, W. Tang, Z.L. Wang, A generalized approach for enhancing contact-electro-catalysis of oxides in a broad temperature range by fluorination, Nat. Commun. 16 (2025) 11035, https://doi.org/10.1038/s41467-025-66002-5.

[55] Z. Chen, Y. Lu, R. Hong, Z. Liang, L. Wen, X. Liu, Q. Liu, Recent progress of solid–liquid interface-mediated contact-electro-catalysis, Langmuir 40 (2024) 5557–5570, https://doi.org/10.1021/acs.langmuir.3c03411.

[56] L. Yang, R. Grzeschik, S. Schlücker, W. Xie, Contact electrification as an emerging strategy for controlling the performance of metal nanoparticle catalysts, Chem. A Eur. J. 30 (2024) e202401718, https://doi.org/10.1002/chem.202401718.

[57] Z.L. Wang, Contact-Electro-Catalysis (CEC), in: Z.L. Wang (Ed.), Contact-Electrification of Matter, Springer Nature Switzerland, Cham, 2025, pp. 279–321.

[58] C. Wang, R. Zhao, W. Fan, L. Li, H. Feng, Z. Li, C. Yan, X. Shao, K. Matyjaszewski, Z. Wang, Tribochemically controlled atom transfer radical polymerization enabled by contact electrification, Angew. Chem. Int. Ed. 62 (2023) e202309440, https://doi.org/10.1002/anie.202309440.

[59] X. Chen, Y. Xia, Y. Yang, Y. Xu, X. Jia, R. N. Zare, F. Wang, Microdroplet-mediated multiphase cycling in a cloud of water drives chemoselective electrolysis, J. Am. Chem. Soc. 146 (2024) 29742–29750, https://doi.org/10.1021/jacs.4c11224.

[60] F. Yin, J.-H. Liu, Y. Zhang, M.-N. Liu, L.-Y. Wang, Z.-C. Yu, W.-H. Yang, J. Zhang, Y.-Z. Long, Contact-electro-catalysis for organic pollutants degradation based on 2D fluorinated graphite, Adv. Funct. Mater. 34 (2024) 2406417, https://doi.org/10.1002/adfm.202406417.

[61] Z. Chen, Y. Lu, X. Liu, J. Li, Q. Liu, Novel magnetic catalysts for organic pollutant degradation via contact electro-catalysis, Nano Energy 108 (2023) 108198, https://doi.org/10.1016/j.nanoen.2023.108198.

[62] K. Li, Y. Lai, S. Lin, L. Zhou, M. He, H. Lin, Y. Yuan, Contact-Electro-Catalysis for the Degradation of Pentachlorophenol Using Inert Fluorinated Ethylene Propylene Powders, ACS ES&T Eng. 4 (2024) 2485–2494, https://doi.org/10.1021/acsestengg.4c00284.

[63] J. Xu, X. Song, Y. Lu, L. Lyu, C. Basheer, R.N. Zare, Intrinsic Electric Field Triggers Phenol Oxidative Degradation at Microbubble Interfaces, J. Am. Chem. Soc. (2025), https://doi.org/10.1021/jacs.5c16083.

[64] Y. Chen, H. Li, Y. Su, X. Dong, W. Tang, Contact-electro-catalysis for the degradation of 4-chlorophenol using pristine dielectric powders, Sep. Purif. Technol. 360 (2025) 131112, https://doi.org/10.1016/j.seppur.2024.131112.

[65] D.-Q. Cao, R.-K. Fang, Y.-X. Song, M.-G. Ma, H. Li, X.-D. Hao, R. Wu, X. Chen, Contact-electro-catalysis for degradation of trace antibiotics in wastewater, Chem. Eng. J. 487 (2024) 150531, https://doi.org/10.1016/j.cej.2024.150531.

[66] R. Wang, S. Wang, B. Du, X. Bai, D. Gao, X. Ren, W. Guo, G. Chen, Self-powered monitoring and synergistic peroxymonosulfate activation via Janus-structured PVDF@Cu for enhanced levofloxacin degradation, Chem. Eng. J. 519 (2025) 164970, https://doi.org/10.1016/j.cej.2025.164970.

[67] H. Yang, X. Jing, P. Ju, M. Guo, P. Guan, H. Yu, Y. Wan, H. Zeng, J. Wang, H. Xie, K. Hu, Contact-electro-catalysis with rare-earth oxides for antibiotic degradation and direct synthesis of H2O2, J. Hazard. Mater. 501 (2026) 140875, https://doi.org/10.1016/j.jhazmat.2025.140875.

[68] S. Ye, B. Xiang, Z. Chen, H. Wang, L. Wen, Y. Luo, Z. Chen, Y. Lu, Q. Liu, Z. Chen, Boosting contact electro-catalysis efficiency via nano-confinement effect in organic wastewater degradation, Nano Energy 136 (2025) 110702, https://doi.org/10.1016/j.nanoen.2025.110702.

[69] D. Ma, J. Zhang, W. Li, J. Ma, K. He, K. Yang, J. Cui, Q. Liu, S. Lv, M. Zhang, F. Cheng, D. Xing, FeIII-driven self-cycled Fenton via contact-electro-catalysis for water purification, npj Clean. Water 8 (2025) 42, https://doi.org/10.1038/s41545-025-00476-0.

[70] L. Li, J. Wu, A. Xia, X. Zhu, Q. Liao, Tandem Mechano-Enzymatic Catalysis: A Green Revolution in Lignocellulosic Biomass Pretreatment via Contact-Electro-Catalysis, ACS Sustain. Chem. & Eng. 13 (2025) 8508–8514, https://doi.org/10.1021/acssuschemeng.5c01557.

[71] H. Jiang, F. Yang, R. Wang, G. Zhu, Y. Zhao, Synergistic contact-electro-catalysis using independent plastic types for emerging contaminants removal and resource valorization, Chem. Eng. Sci. 323 (2026) 123240, https://doi.org/10.1016/j.ces.2025.123240.
[72] R. Ying, M. Ma, X. Zhao, Y. Dong, X. Zhang, Z. Gao, Ultrafast Degradation of Organic Dyes by Water Atomization and Contact-Electro-Catalysis, Langmuir 41 (2025) 10434–10442, https://doi.org/10.1021/acs.langmuir.5c00337.
[73] L.-Y. Wang, J.-H. Liu, M.-N. Liu, F. Yin, Z.-C. Yu, M.-J. Li, Y. Zhang, H.-D. Zhang, J. Zhang, Y.-Z. Long, Contact-electro-catalytic degradation of organic dyes based on solid-liquid-solid friction, Nano Energy 128 (2024) 109910, https://doi.org/10.1016/j.nanoen.2024.109910.
[74] X.-F. Li, A. Berbille, T.-Y. Wang, X. Zhao, S. Li, Y. Su, H. Li, G. Zhang, Z. Wang, L. Zhu, J. Liu, Z.L. Wang, Defect Passivation Toward Designing High-Performance Fluorinated Polymers for Liquid–Solid Contact-Electrification and Contact-Electro-Catalysis, Adv. Funct. Mater. 34 (2024) 2315817, https://doi.org/10.1002/adfm.202315817.
[75] W. Li, J. Tu, J. Sun, Y. Zhang, J. Fang, M. Wang, X. Liu, Z.-Q. Tian, F. Ru Fan, Boosting Reactive Oxygen Species Generation via Contact-Electro-Catalysis with FeIII-Initiated Self-cycled Fenton System, Angew. Chem. Int. Ed. 64 (2025) e202413246, https://doi.org/10.1002/anie.202413246.
[76] Y. Zhang, T. Kang, X. Han, W. Yang, W. Gong, K. Li, Y. Guo, Molecular-functionalized metal-organic frameworks enabling contact-electro-catalytic organic decomposition, Nano Energy 111 (2023) 108433, https://doi.org/10.1016/j.nanoen.2023.108433.
[77] Z. Liang, W. Li, J. Tu, F.R. Fan, Mechanically Induced Contact-Electro-Catalysis: Free Radical Generation, Reaction Pathways, and Catalytic Applications, ChemCatChem 17 (2025) e202500282, https://doi.org/10.1002/cctc.202500282.
[78] I.-Y. Suh, J. Jeon, M.J. Park, H. Ryu, Y.J. Park, S.-W. Kim, Recent Studies on Solid–Liquid Contact Electrification, ACS Appl. Electron. Mater. 6 (2024) 4826–4842, https://doi.org/10.1021/acsaelm.4c00531.
[79] H. Zhang, K. Wang, J. Li, J. Li, R. Zhang, Y. Zheng, Liquid-based nanogenerator fabricated by a self-assembled fluoroalkyl monolayer with high charge density for energy harvesting, Matter 5 (2022) 1466–1480, https://doi.org/10.1016/j.matt.2022.02.013.
[80] M. Zheng, Z. Hu, T. Liu, M. Sperandio, E.I.P. Volcke, Z. Wang, X. Hao, H. Duan, S. E. Vlaeminck, K. Xu, Z. Zuo, J. Guo, X. Huang, G.T. Daigger, W. Verstraete, M.C. M. van Loosdrecht, Z. Yuan, Pathways to advanced resource recovery from sewage, Nat. Sustain 7 (2024) 1395–1404, https://doi.org/10.1038/s41893-024-01423-6.
[81] R. Wang, G. Zhang, L. Liu, Q. Ji, H. Lan, J. Qu, H. Liu, Hierarchical Ru0/Ruδ+/Al2O3 electrocatalyst enabling phenolic contaminant-to-chemical conversion, Nat. Commun. 16 (2025) 10356, https://doi.org/10.1038/s41467-025-65330-w.
[82] F. Dong, B. Xu, X. Ma, T. Liu, B. Luo, X. Li, S. Song, S. Nie, Advanced Tribioelectric Materials for Contact Electrocatalytic Degradation of Pollutants, Small 21 (2025) 2500369, https://doi.org/10.1002/smll.202500369.
[83] D. Xu, R. Chen, Standards needed for antibiotics in water, 1499-1499, Science 377 (2022), https://doi.org/10.1126/science.ade6856.
[84] B. Daisley, C.V. Macpherson, D.J.L. Brettingham, A.E. Moore, G.J. Thompson, E. Allen-Vercoe, Impacts of antibiotic use, air pollution and climate on managed honeybees in Canada, Nat. Sustain 8 (2025) 1087–1099, https://doi.org/10.1038/s41893-025-01603-y.
[85] Y.-W. Li, X.-L. Wu, C.-H. Mo, Y.-P. Tai, X.-P. Huang, L. Xiang, Investigation of Sulfonamide, Tetracycline, and Quinolone Antibiotics in Vegetable Farmland Soil in the Pearl River Delta Area, Southern China, J. Agric. Food Chem. 59 (2011) 7268–7276, https://doi.org/10.1021/jf1047578.
[86] L. Huang, H. Liu, T.C. Zhang, Y. Wang, S. Yuan, Peroxymonosulfate-Assisted BiVO4/Exfoliated g-C3N4 Heterojunction for High-Performance Photodegradation of Tetracycline Induced by Visible Light, Ind. Eng. Chem. Res. 61 (2022) 16418–16430, https://doi.org/10.1021/acs.iecr.2c02458.
[87] Y. Chen, Y. Huang, Y. Chen, Y. Li, N. Sidikjan, N. Lin, Y. Li, X. Guo, G. Shen, M. Liu, A systematic review of sources, occurrence, behavior and risks of global marine antibiotics, npj Emerg. Contam. 1 (2025) 15, https://doi.org/10.1038/s44454-025-00015-z.
[88] D. Cocker, T. Mwapasa, R. Grabic, K. Grabicová, A.V. Staňová, K. Chidziwisano, A.P. Roberts, T. Morse, N.A. Feasey, A.C. Singer, Environmental hazards from pollution of antibiotics and resistance-driving chemicals in an urban river network from Malawi, npj Antimicrob. Resist. 3 (2025) 85, https://doi.org/10.1038/s44259-025-00149-5.
[89] C. Liu, L. Zhao, J. Li, J. Wang, H. Xu, X. Chen, J. Qi, C. Sun, Z. Zhu, Y. Wang, F. Meng, Peroxymonosulfate activation by low-cost modified rubber during contact electrification for antibiotics efficient degradation at circumneutral pH: Mechanism and toxicity assessment, Chem. Eng. Sci. 285 (2024) 119642, https://doi.org/10.1016/j.ces.2023.119642.
[90] S. Li, H. Qian, J. Xu, Z.L. Wang, R.N. Zare, D. Wei, Bromophenol blue degradation by contact-electro-catalysis, J. Electroanal. Chem. 1007 (2026) 119942, https://doi.org/10.1016/j.jelechem.2026.119942.
[91] H. Liu, Y. Wang, Contact-Electro-Catalysis-Assisted Separation via a Dancing PTFE Membrane for Fouling Control, ACS Appl. Mater. Interfaces 16 (2024) 1826–1836, https://doi.org/10.1021/acsami.3c14746.
[92] H. Li, A. Xie, C. Hong, Z. Wang, X. Chu, Z.L. Wang, Y. Liu, P. Jiang, Hydroxyl radical generation from H2O2via liquid–liquid contact-electro-catalysis, Chem. Sci. 16 (2025) 20580–20593, https://doi.org/10.1039/D5SC05862G.
[93] Z. Chen, Y. Zhang, P. Lv, T. Wu, J. He, J. Du, Q. Sun, Q. Wu, J. Yang, Y. Zhang, Y. Zhang, F. He, C. Cui, G. Hong, H. Zhu, Y. Li, J. Guo, X. Deng, Hand-powered interfacial electric-field-enhanced water disinfection system, Nat. Nanotechnol. (2025), https://doi.org/10.1038/s41565-025-02033-9.
[94] L. Dong, X. Sun, W. Li, J. Liu, T. Hou, Q. Bie, W. Dong, C. Hou, S. Chen, Interfacial Water Harvesting from Air via MIL-101(Cr)@LiCl-Doped Hydrogel for Contact-Electro-Catalytic Antibacterial and Hydrogen Production, Small 21 (2025) e05598, https://doi.org/10.1002/smll.202505598.
[95] P. Wei, M. Tang, Y. Wang, B. Hu, X. Qu, Y. Wang, G. Gao, Low-frequency ultrasound assisted contact-electro-catalysis for efficient inactivation of Microcystis aeruginosa, J. Hazard. Mater. 478 (2024) 135537, https://doi.org/10.1016/j.jhazmat.2024.135537.
[96] H. Li, Z. Wang, X. Chu, Y. Zhao, G. He, Y. Hu, Y. Liu, Z.L. Wang, P. Jiang, Free Radicals Generated in Perfluorocarbon–Water (Liquid–Liquid) Interfacial Contact Electrification and Their Application in Cancer Therapy, J. Am. Chem. Soc. 146 (2024) 12087–12099, https://doi.org/10.1021/jacs.4c02149.
[97] J. Zhang, Y. Fan, Y. Wang, X. Wang, Z. Wang, H. Liu, C. Liu, Z.L. Wang, D. Luo, Contact-electro-catalysis therapy combats tumors by activating the immune system and blocking extracellular vesicles-mediated metastasis, Nano Energy 145 (2025) 111431, https://doi.org/10.1016/j.nanoen.2025.111431.
[98] X. Zhang, S. Cheng, C. Chen, X. Wen, J. Miao, B. Zhou, M. Long, L. Zhang, Keto-anthraquinone covalent organic framework for H2O2 photosynthesis with oxygen and alkaline water, Nat. Commun. 15 (2024) 2649, https://doi.org/10.1038/s41467-024-47023-y.
[99] Y. Wang, P. Wei, Z. Shen, C. Wang, J. Ding, W. Zhang, X. Jin, C.D. Vecitis, G. Gao, O2-Independent H2O2 Production via Water–Polymer Contact Electrification, Environ. Sci. Technol. 58 (2024) 925–934, https://doi.org/10.1021/acs.est.3c07674.
[100] B. Chen, Y. Xia, R. He, H. Sang, W. Zhang, J. Li, L. Chen, P. Wang, S. Guo, Y. Yin, L. Hu, M. Song, Y. Liang, Y. Wang, G. Jiang, R.N. Zare, Water–solid contact electrification causes hydrogen peroxide production from hydroxyl radical recombination in sprayed microdroplets, P. Natl. Acad. Sci. USA 119 (2022) e2209056119, https://doi.org/10.1073/pnas.2209056119.
[101] Z. Liu, X. Jiang, X. Cheng, Y. Pei, X. Wei, W. Han, W. Tang, Z.L. Wang, Catalytic Effect of Gray Gallium Nitride for Hydrogen Peroxide Generation: Insights into Mechanical Stimuli-Driven Semiconductor–Liquid Interface Alteration, ACS Nano 19 (2025) 33361–33371, https://doi.org/10.1021/acsnano.5c09730.
[102] A. Berbille, X. Li, Y. Su, S. Li, X. Zhao, L. Zhu, Z.L. Wang, Mechanism for generating H2O2 at water-solid interface by contact-electrification, Adv. Mater. 35 (2023) 2304387, https://doi.org/10.1002/adma.202304387.
[103] J. Zhao, X. Zhang, J. Xu, W. Tang, Z. Lin Wang, F. Ru Fan, Contact-electro-catalysis for Direct Synthesis of H2O2 under Ambient Conditions, Angew. Chem. Int. Ed. 62 (2023) e202300604, https://doi.org/10.1002/anie.202300604.
[104] Y. Wang, Y. Wang, B. Hu, M. Qiu, G. Gao, P. Wei, Catalyst-free contact-electro-catalytic H2O2 synthesis via simple combination of a poly(tetrafluoroethylene) stir bar and ultrasound, Chem. Commun. 60 (2024) 7331–7334, https://doi.org/10.1039/D4CC01576B.
[105] S. Lin, D.-K. Ma, H. Zhou, H. Yuan, C. Wan, X. Hu, Enhanced hydrogen peroxide photosynthesis achieved over resorcinol formalde resin/polytetrafluoroehtylene through contact electrification, Appl. Catal. A Gen. 709 (2026) 120671, https://doi.org/10.1016/j.apcata.2025.120671.
[106] K. Lee, S. Bose, X. Song, S.Q. Choi, R.N. Zare, Continuous flow contact electrocatalysis for hydrogen peroxide production, J. Phys. Chem. C 129 (2025) 6254–6261, https://doi.org/10.1021/acs.jpcc.5c00163.
[107] N. Wang, W. Jiang, J. Yang, H. Feng, Y. Zheng, S. Wang, B. Li, J.Z.X. Heng, W. C. Ong, H.R. Tan, Y.-W. Zhang, D. Wang, E. Ye, Z. Li, Contact-electro-catalytic CO2 reduction from ambient air, Nat. Commun. 15 (2024) 5913, https://doi.org/10.1038/s41467-024-50118-1.
[108] K. Shi, H. Meng, J. Liu, S. Ma, W. Tang, Synergistic Contact-Electro-Catalysis and Photocatalysis via TiO2@PTFE Composites for Efficient N2 to NH3 Conversion, Angew. Chem. Int. Ed. n/a, e202515707, ⟨https://doi.org/10.1002/anie.202515707⟩.
[109] T. Jia, W. Wang, C. Zhang, L. Zhang, W. Wang, Polydopamine-mediated contact-electro-catalysis for efficient partial oxidation of methane, Angew. Chem. Int. Ed. 64 (2025) e202413343, https://doi.org/10.1002/anie.202413343.
[110] Y.-W. Zhou, E. Ibáñez-Alé, N. López, B. Roldan Cuenya, C.S. Kley, Carbonate anions and radicals induce interfacial water ordering in CO2 electroreduction on gold, Nat. Chem. (2025), https://doi.org/10.1038/s41557-025-01977-8.
[111] P. Jin, P. Guo, N. Luo, H. Zhang, C. Ni, R. Chen, W. Liu, R. Li, J. Xiao, G. Wang, F. Zhang, P. Fornasiero, F. Wang, Photochemical H2 dissociation for nearly quantitative CO2 reduction to ethylene, Science 389 (2025) 1037–1042, https://doi.org/10.1126/science.adq3445.
[112] J. Wu, Y. Shao, F. Xing, B. Chen, L. Huang, W. Li, Y. Shi, Direct conversion of N2 by contact-electrocatalysis (CEC): a highly efficient dual-pathway approach for tunable co-production of nitrate and ammonia, Nano Energy 148 (2026) 111661, https://doi.org/10.1016/j.nanoen.2025.111661.
[113] S. Huang, Y. Liu, L. Ren, L. Huang, J. Tang, Z. Yu, M. Chen, S. Zhou, Direct conversion of N2 to nitric acid via contact electrocatalysis, ACS Sustain. Chem. & Eng. 13 (2025) 10486–10494, https://doi.org/10.1021/acssuschemeng.5c02290.
[114] J. Li, Y. Xia, X. Song, B. Chen, R.N. Zare, Continuous ammonia synthesis from water and nitrogen via contact electrification, P. Natl. Acad. Sci. USA 121 (2024) e2318408121, https://doi.org/10.1073/pnas.2318408121.
[115] N. Wang, W. Jiang, H. Feng, J. Yang, B. Li, T. Yu, C. Du, J. Wang, J.Z.X. Heng, J. H. Pan, Y.-W. Zhang, D. Wang, E. Ye, Z. Li, Target high-efficient ethylene production from dilute CO2 enabled by sustainable contact electrons, Small 21 (2025) 2411815, https://doi.org/10.1002/smll.202411815.
[116] X. Li, Z. Yu, N. Wu, Y. Sun, X. Chen, Y. Zhang, S. Qin, X. Wang, H. Gong, Z. Meng, M. Willatzen, N. Li, Z.L. Wang, Z. Bian, X. Chen, Largely Enhanced Photocatalysis

Process by Contact-Electro-Catalysis for Efficient and Eco-Friendly Recovery of Gold, Adv. Mater. n/a, e14244, ⟨https://doi.org/10.1002/adma.202514244⟩.
[117] Z. Zhou, S. Zhang, D. Song, J. Cao, Y. Qiu, C. Xue, H. Xu, J. Mei, Plasmonic silver particles reduced by contact-electro-catalysis with acoustic-solid interaction mechanism for enhancing SERS detection, J. Environ. Chem. Eng. 13 (2025) 120102, https://doi.org/10.1016/j.jece.2025.120102.
[118] H. Yan, X. Song, S. Li, J. Li, J. Zhang, Y. Zhang, L. Zhang, Contact-electro-catalysis enables ultrasonic synthesis of gold nanoparticles at water–PTFE interfaces, ChemNanoMat 11 (2025) e202500050, https://doi.org/10.1002/cnma.202500050.
[119] M. Shah, S. Li, Z. Yang, J. Liu, P. Peng, H. Qian, Z.L. Wang, D. Wei, Synergistic effects in triboelectric charge-driven redox reactions, Nano Energy 144 (2025) 111380, https://doi.org/10.1016/j.nanoen.2025.111380.
[120] X. Shen, S. Wang, L. Zhao, H. Song, W. Li, C. Li, S. Lv, G. Wang, Simultaneous Cu (II)-EDTA decomplexation and Cu(II) recovery using integrated contact-electro-catalysis and capacitive deionization from electroplating wastewater, J. Hazard. Mater. 472 (2024) 134548, https://doi.org/10.1016/j.jhazmat.2024.134548.
[121] Z. Chen, S. Li, K. Feng, Z. Wen, J. Zhong, Promoting Co(ii)–EDTA decomplexation by central atom oxidation in contact-electro-catalysis, Phys. Chem. Chem. Phys. 27 (2025) 15742–15748, https://doi.org/10.1039/D5CP01566A.
[122] H. Li, A. Berbille, X. Zhao, Z. Wang, W. Tang, Z.L. Wang, A contact-electro-catalytic cathode recycling method for spent lithium-ion batteries, Nat. Energy 8 (2023) 1137–1144, https://doi.org/10.1038/s41560-023-01348-y.
[123] B.K. Biswal, B. Zhang, P. Thi Minh Tran, J. Zhang, R. Balasubramanian, Recycling of spent lithium-ion batteries for a sustainable future: recent advancements, Chem. Soc. Rev. 53 (2024) 5552–5592, https://doi.org/10.1039/D3CS00898C.
[124] M. Yang, S. Qin, Y. Yang, M. Wu, T. Lei, Y. Liu, H. Shao, A green and efficient strategy for leaching critical metals from spent LiNixCoyMnzO2 cathodes: modulating the dielectric SiO2 contact-electro-catalytic activity, Green. Chem. (2026), https://doi.org/10.1039/D5GC04080A.
[125] H. Li, Z. Cui, Y. Chen, W. Tang, Reusable Fe3O4@SiO2 contact-electro-catalysis for recycling valuable metal from spent lithium-ion batteries, Chem. Eng. Sci. 320 (2026) 122350, https://doi.org/10.1016/j.ces.2025.122350.
[126] B. Niu, Z. Xu, J. Xiao, Y. Qin, Recycling hazardous and valuable electrolyte in spent lithium-ion batteries: urgency, progress, challenge, and viable approach, Chem. Rev. 123 (2023) 8718–8735, https://doi.org/10.1021/acs.chemrev.3c00174.
[127] B. Zhang, X. Hu, R. Zhang, J. Wang, X. Li, B. Huang, M. Hu, L. He, Z. Zhao, L. Zhou, J. Wang, Z.L. Wang, Recycling Spent Lithium Iron Phosphate via Contact-Electro-Catalysis, Advanced Energy Materials n/a, e03508, ⟨https://doi.org/10.1002/aenm.202503508⟩.
[128] L. Chen, Y. Fan, N. Jiang, X. Huang, M. Yu, H. Zhang, Z. Xu, D. He, Y. Wang, C. Ding, X. Wu, C. Li, S. Zhang, H. Liu, X. Shi, F. Zhang, T. Zhang, D. Luo, C. Wang, Y. Liu, An energy metabolism-engaged nanomedicine maintains mitochondrial homeostasis to alleviate cellular ageing, Nat. Nanotechnol. (2025), https://doi.org/10.1038/s41565-025-01972-7.
[129] Y. Liu, S. Ni, W. Yao, W. Wang, Y. Zhao, J. Zhang, H. Liu, L. Yang, Self-cleaning contact-electro catalyst for uranium extraction from seawater, Chem. Eng. J. 522 (2025) 167604, https://doi.org/10.1016/j.cej.2025.167604.
[130] Z. Dai, L. Chen, B. Liang, L. Li, D. Ding, Efficient extraction of uranium(VI) in aqueous solution by contact-electro-catalysis, Chem. Eng. J. 502 (2024) 157893, https://doi.org/10.1016/j.cej.2024.157893.
[131] C. Xu, S. Li, Z. Yang, M. Willatzen, Z. Lin Wang, D. Wei, Contact-electro-luminescence triggered by triboelectric charge, Chem. Eng. J. 501 (2024) 157754, https://doi.org/10.1016/j.cej.2024.157754.
[132] D. Zhong, H. Li, Y. Yang, X. Huang, Z. Yang, C. Wang, Contact-electro-catalysis of polytetrafluoroethylene particles for luminol electrochemiluminescence/sonochemiluminescence and its application for detecting superoxide dismutase and thiabendazole, Sens. Actuators B Chem. 446 (2026) 138714, https://doi.org/10.1016/j.snb.2025.138714.
[133] C. Xu, S. Li, Y. Zhang, Z. Wang, Z.L. Wang, D. Wei, Contact-electro-chemistry induced by flow electrification in dielectric tubes, Nano Energy 134 (2025) 110526, https://doi.org/10.1016/j.nanoen.2024.110526.
[134] W. Li, J. Song, Z. Liang, J. Liu, Y. Lin, J.-M. Zhou, Y.-H. Ruan, F.R. Fan, Innovative undergraduate experiments in solid–liquid contact electrification: droplet nanogenerators and contact-electro-catalysis, J. Chem. Educ. 102 (2025) 1662–1668, https://doi.org/10.1021/acs.jchemed.4c01263.
[135] Y. Wang, Y. Zhang, H. Li, Y. Feng, J. Ma, C. Ban, A. Cesnokovs, X. Wang, L. Ruan, S. Jing, L. Cao, Y. Niu, Y. Chen, C. Ma, Theory-assisted design of transition-metal-doped Bi5O7I for efficient contact-electro-catalytic hydrogen evolution, Chem. Eng. J. 528 (2026) 172290, https://doi.org/10.1016/j.cej.2025.172290.
[136] N. Tian, J. Kuang, C. Yuan, X. Zhang, Y. Zhang, H. Huang, Direct hydrogen production from pure water through contact-electro-catalysis, J. Mater. Chem. A 13 (2025) 32344–32350, https://doi.org/10.1039/D5TA03134F.
[137] Z. Wang, X. Dong, F.-J. Lv, W. Tang, A perspective on contact-electro-catalysis based on frontier molecular orbitals, Mater. Adv. 5 (2024) 6373–6377, https://doi.org/10.1039/D4MA00514G.
[138] M.-N. Liu, J.-H. Liu, L.-Y. Wang, F. Yin, G. Zheng, R. Li, J. Zhang, Y.-Z. Long, Strategies for improving contact-electro-catalytic efficiency: a review, Nanomaterials 15 (2025) 386.
[139] X. Li, W. Tong, Contact-electro-catalysis under natural and industrial conditions: mechanisms, strategies, and challenges, J. Mater. Chem. A 12 (2024) 19783–19805, https://doi.org/10.1039/D4TA02062F.
[140] Y. Jiang, H. Yu, X. Chen, L. Wu, Z. Fang, P.E. Tsang, Research progress of contact-electro-catalysis in the remediation of emerging pollutants: exploration from mechanism to application, Environ. Res. 285 (2025) 122705, https://doi.org/10.1016/j.envres.2025.122705.
[141] S. Li, Z.L. Wang, D. Wei, Chemical reactions at electrified interfaces, Acc. Chem. Res. 59 (2026) 285–297, https://doi.org/10.1021/acs.accounts.5c00735.
[142] S. Li, Z.L. Wang, D. Wei, Hidden interfacial electric fields in chemistry: contact electrification and beyond, Chem. Soc. Rev. (2026), https://doi.org/10.1039/D5CS01066G.

Han Qian achieved the B.S. degree from Henan University of Science and Technology in 2023. He continues pursuing Ph.D. degree in Beijing Institute of Nanoenergy and Nanosystems, Chinese Academy of Sciences. He focuses on the transfer of ions and electrons at interfaces, with the applicatons in iontronics, osmotic energy conversion, and contact-electro-chemistry (CE-Chemistry).

Prof. Zhong Lin Wang received his Ph.D. from Arizona State University in physics. He now is the Hightower Chair in Materials Science and Engineering, Regents' Professor, Engineering Distinguished Professor and Director, Center for Nanostructure Characterization, at Georgia Tech. Dr. Wang has made original and innovative contributions to the synthesis, discovery, characterization and understanding of fundamental physical properties of oxide nanobelts and nanowires, as well as applications of nanowires in energy sciences, electronics, optoelectronics and biological science. His discovery and breakthroughs in developing nanogenerators established the principle and technological road map for harvesting mechanical energy from environment and biological systems for powering personal electronics. His research on self-powered nanosystems has inspired the worldwide effort in academia and industry for studying energy for micro-nano-systems, which is now a distinct disciplinary in energy research and future sensor networks. He coined and pioneered the field of piezotronics and piezophototronics by introducing piezoelectric potential gated charge transport process in fabricating new electronic and optoelectronic devices. Details can be found at: http://www.nanoscience.gatech.edu

Prof. Di Wei serves as the Principal Investigator at BINN and heads the Iontronics Laboratory. As Fellow of the Royal Society of Chemistry (FRSC) and Senior Member of Wolfson College at Cambridge University, he has published over 150 papers including Nat. Energy, Nat. Commun., Sci. Adv., PNAS, Joule, Matter, Adv. Mater., Angew. Chem. Int. Ed., J. Am. Chem. Soc., Energ. Environ. Sci., Chem. Soc. Rev. etc. as the first/corresponding author. Prof. Wei also has a portfolio of over 200 international patents (including PCT). Notably, 92 patents have been successfully granted, many of which have been transferred to leading companies like Nokia in Finland and Lyten in the USA. Additionally, Prof. Wei has edited 3 English books, published by Wiley and Cambridge University Press etc., focusing on nanotechnology for energy and information technology. His achievements have been recognized by the first prize of the Nokia Global Innovation and Excellence Award, Brian Conway Prize in Physical Electrochemistry from the International Society of Electrochemistry (ISE) and various other prizes from ISE and RSC. Details can be found at: http://iontronics.group/en/